



Original article

Design, synthesis and biological evaluation of new classes of thieno [3,2-*d*]pyrimidinone and thieno[1,2,3]triazine as inhibitor of vascular endothelial growth factor receptor-2 (VEGFR-2)



Enrico Perspicace^a, Valérie Jouan-Hureau^d, Rino Ragno^{b,*}, Flavio Ballante^b, Stefania Sartini^c, Concettina La Motta^c, Federico Da Settimo^c, Binbin Chen^a, Gilbert Kirsch^a, Serge Schneider^e, Béatrice Faivre^d, Stéphanie Hesse^{a,**}

^a Laboratoire d'Ingénierie Moléculaire et Biochimie Pharmacologique, UMR CNRS 7565 SRS MC, Institut Jean Barriol, FR CNRS 2843, Université de Lorraine, 1 Boulevard Arago, 57070 Metz, France

^b Rome Center for Molecular Design, Dipartimento di Chimica e Tecnologie del Farmaco, Università degli Studi di Roma "La Sapienza", P. le A. Moro 5, 00185 Roma, Italy

^c Dipartimento di Farmacia, Università di Pisa, Via Bonanno 6, 56126 Pisa, Italy

^d EA 4421 SIGReTO, Université de Lorraine, Faculté de pharmacie, 5-7 Rue Albert Lebrun, BP80403, 54001 Nancy cedex, France

^e Laboratoire National de Santé, Division de Toxicologie, Université de Luxembourg, 162a Avenue de la Faïencerie, L-1511 Luxembourg, Luxembourg

ARTICLE INFO

Article history:

Received 13 December 2012

Received in revised form

7 March 2013

Accepted 10 March 2013

Available online 19 March 2013

Keywords:

Vascular endothelial growth factor receptor-2 (VEGFR-2)

Anti-angiogenic activity

Structure-based drug design (SBDD)

Ligand-based drug design (LBDD)

3-D QSAR

Thieno[3,2-*d*]pyrimidinone

Thieno[1,2,3]triazine

Endothelial cell tube formation

ABSTRACT

Driven by a multidisciplinary approach combination (Structure-Based (SB) Three-Dimensional Quantitative Structure–Activity Relationships (3-D QSAR), molecular modeling, organic chemistry and various biological evaluations) here is reported the disclosure of new thienopyrimidines **1–3** as inhibitors of KDR activity and human umbilical vein endothelial cell (HUVEC) proliferation. More specifically, compound **2f** represents a new lead compound that inhibits VEGFR-2 and HUVEC at μM concentration. Moreover by the mean of an endothelial cell tube formation *in vitro* model **2f** tartaric acid salt proved to block angiogenesis of HUVEC at μM level.

© 2013 Elsevier Masson SAS. All rights reserved.

1. Introduction

Angiogenesis, the process of new blood vessels formation, creating new capillaries from existing vasculature, is a normal process for organ development. It occurs especially during embryogenesis, in development and homeostasis of adult tissues, in wound repair and in the menstrual cycle [1,2]. It's an essential and highly regulated process under physiological conditions. When a

malfunction in controlling mechanisms of angiogenesis occurs, it may be involved in the development and progression of various diseases such as rheumatoid arthritis [3], inflammation [4], ocular neovascularization [5], psoriasis [6], tumor growth [7] and metastasis [8]. More than twenty different factors are involved in this process, among which the vascular endothelial growth factors (VEGFs) [9–11]. The VEGF family includes VEGF-A (usually named VEGF), VEGF-B, VEGF-C, VEGF-D, VEGF-E, VEGF-F and a structurally related molecule, Placental Growth Factor (PlGF). Three high-affinity VEGF tyrosine kinase receptors have been identified: VEGFR-1 (Flt-1), VEGFR-2 (KDR) and VEGFR-3 (Flt-4). VEGF and its receptors represent one of the best-validated signaling pathways in angiogenesis [12]. Furthermore, disruption of VEGFR-2 signaling has resulted in inhibition of angiogenesis and without new blood vessels

* Corresponding author. Tel.: +39 6 4991 3937; fax: +39 6 4991 3627.

** Corresponding author. Tel.: +33 3 8754 7197; fax: +33 3 8731 5801.

E-mail addresses: rino.ragno@uniroma1.it (R. Ragno), stephanie.hesse@univ-lorraine.fr (S. Hesse).

to supply oxygen, nutrients and catabolic products, tumor cells could not proliferate and thus are likely to remain dormant [13,14]. Therefore, VEGFR-2 has been the principal target of anti-angiogenic therapies [15–18], although additional studies have underlined the importance of signaling through VEGFR-1 [19].

In recent years, many molecules have been described on their ability to inhibit angiogenesis. For example, the recombinant humanized monoclonal antibody bevacizumab (Avastin®, Genentech) recognizes and blocks VEGF [20], and was the first anti-angiogenic agent to be approved by Food and Drug Administration (FDA). Other inhibitory molecules have been developed targeting the vascular endothelial growth factor receptors (Figs. 1 and 2). Sorafenib (BAY 43-9006 or Nexavar®) is a derivative initially selected as an inhibitor of Raf kinase by targeting MAPK pathway but this compound has also a powerful inhibitory action on VEGFR-1, VEGFR-2, and Platelet Derived Growth Factor Receptor- β (PDGFR- β) [21]. Sunitinib (SU 011248 or Sutent®) is an oral multi-targeted receptor tyrosine kinase (RTK) which inhibits VEGFR-1, VEGFR-2, PDGFR, KIT, Flt3 and the receptor encoded by the RET proto-oncogene [22]. Today, targeting tumor angiogenesis has become part of daily care for many solid tumors. Indeed, survival gains were achieved in the case of metastatic renal cell carcinoma and hepatocarcinoma for which medical treatment had little or no effect. However, numerous side effects have been reported (skin, cardiovascular) [23,24] to which the clinician had not been confronted with the molecules of conventional chemotherapy. Furthermore, studies have shown the emergence of resistance mechanisms to anti-angiogenic products [25]. Indeed, in some cases, despite initial sensitivity and a dramatic reduction in volume, treated tumors resumed their growth and invasiveness. Within this scenario it is obvious the continuous need to develop new anti-angiogenic agents that can both reduce the side effects and block resistance of tumor cells. In this study we disclose the new thienopyrimidines **1–3** (Fig. 3) as inhibitors of VEGFR-2 designed by a Structure-Based (SB) Three-Dimensional Quantitative Structure–Activity Relationships (3-D QSAR), molecular modeling and biological combined approach.

2. Results and discussion

2.1. Rationale, preliminary screening and design

Quinazoline [27,28] and naphtamide [29] derivatives have attracted great interest as VEGFR-2 inhibitors over the past years.

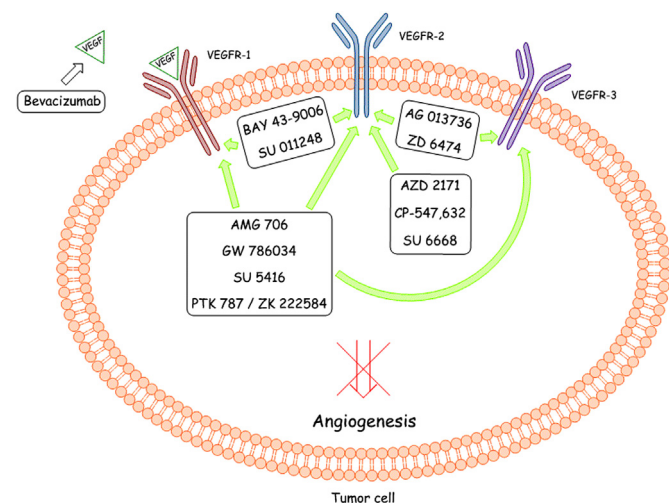


Fig. 1. Inhibition pathways of angiogenesis [26].

Furo[2,3-*d*]pyrimidines [30], pyridinyltriazines [31] and pyrimidinylindazoles [32] were also reported as VEGFR inhibitors. All compounds were comprehensively studied and many of them were co-crystallized in the ATP-binding site of KDR. Such amount of structural information was used by us to develop a predictive SB 3-D QSAR model [33] and herein used as tools to develop new VEGFR-2 inhibitors.

Recently, some of us were deeply interested in the synthesis of thienopyrimidine scaffolds and their functionalization via palladium-catalyzed cross-coupling or nucleophilic aromatic substitution reaction (S_NAr) [34,35]. Furthermore, we also developed the methodology to access to selenolo- and thiazolo-triazine scaffolds [36,37]. Thirty-five compounds, (**4–38**), out of all the available ones, were selected as potential VEGFR-2 inhibitors on the basis of their structural similarity to well-known inhibitors from the literature, and thus submitted to a VEGFR-2 inhibition assay, performed as reported in the Experimental section (Tables 1–3) [38]. IC_{50} values were investigated for compounds showing higher % of inhibition (Table 4) by linear regression analysis of the log–dose response curve, which was generated using at least five concentrations of the inhibitor causing an inhibition between 20% and 80%, with three replicates at each concentration.

At the same time, compounds **4–38** were also investigated by our SB 3-D QSAR protocol [33]. As reported in Tables 1–3, only five (**17–19**, **22**, **23**) out of the 35 assayed compounds were found totally inactive, while four derivatives (**14**, **30**, **33** and **35**) inhibited VEGFR-2 at high percentage (over 73%) and their IC_{50} were determined (Table 4). The SB 3-D QSAR protocol application over predicted compounds **4–38** in the range of 5.82–7.92 pIC_{50} , with an average value of 6.56 (Supplementary material Table SM-1). Besides, the over prediction, the fact that 85% of compound displayed indeed some sort of inhibition activity toward VEGFR-2 (Tables 1–3) proved the calculated data to be in agreement with the experimental. Furthermore, due to the lack of Se parameters, for both dockings and 3-D QSAR calculations the Se containing compounds were modeled as sulfur derivatives. Therefore, some errors of predictions were expected for Se containing derivatives **22–38**.

2-D structures, 3-D QSAR predicted pIC_{50} s and docked conformations of compounds **4–38** are reported in Supplementary material Table SM-1. At a first glance, all the compounds bind preferentially in the very first part of the binding site (left sides of figures in Supplementary material Table SM-1) overlapping the thienopyrimidine (**4–13**), thiazolotriazine (**14–21**) and selenolotriazine (**22–38**) scaffolds mainly with the reference structure (PDB ID 2qu5) central benzimidazole. Regarding thienopyrimidines **4–13**, the increasing sterical hindrance of the third fused cycle seems to increase the molecules/VEGFR-2 interactions (compare **4**, **6**, **8** and **11** binding modes with those of **5**, **7**, **9** and **12** in Supplementary material Table SM-1) in agreement with the lower activities of bicycles **4**, **6**, **8** and **11** than those of the **5**, **7**, **9** and **12** (Table 1). In an opposite way, the increase of steric hindrance is detrimental for the thiazolotriazines **14–21** where the smaller derivative **14** shows the higher activity. Actually, within this series, the insertion of different substituents clearly influence both binding modes and activities of the resulting compounds, although no particular pattern can be drawn out from them. Concerning the selenolotriazines **22–38** (modeled as thienotriazines) their binding modes resemble those of thienopyrimidines **4–13**. In a whole, this first series of compounds (**4–38**) was considered as a sort of fragment library for which both the experimental and prediction were used to select the more interesting scaffolds.

A deeper binding mode analysis was then performed on the most active compounds **14**, **30**, **33** and **35** and their conformations as docked by AutoDock revealed that all the four compounds bind roughly in the same region defined by Val27, Ala45, Lys47, Val93,

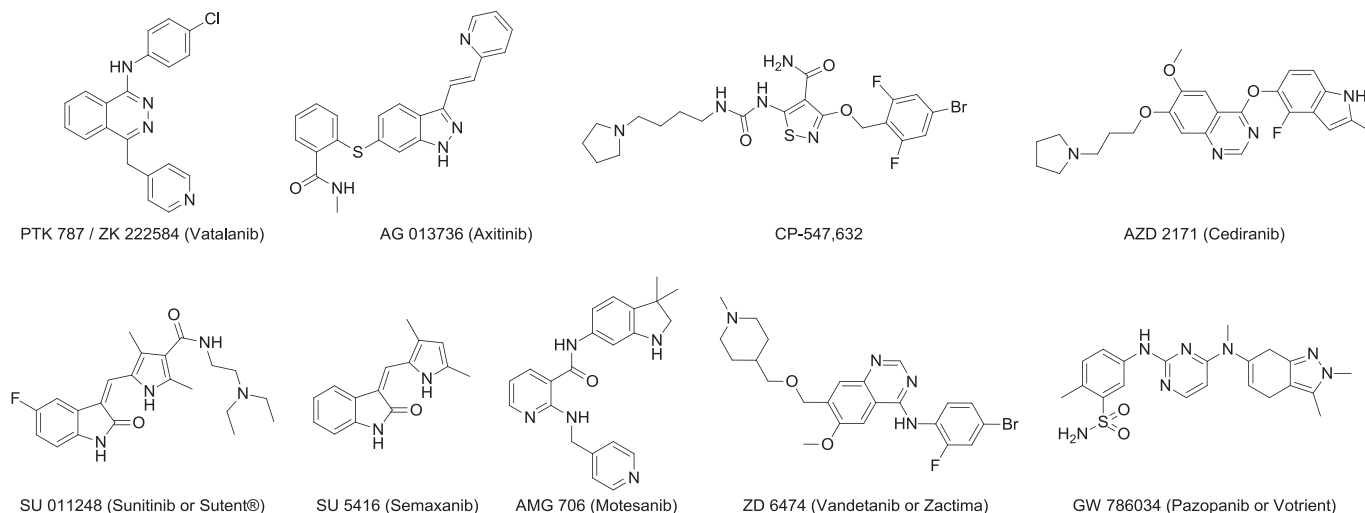


Fig. 2. Examples of anti-angiogenic compounds.

Val95, Leu164 and Phe176 (Fig. 4 and Supplementary material Figure SM-1). While **14**, **30** and **33** shared a common binding mode with the thiazolotriazine/selenolotriazine groups overlapping with the same orientation, on the contrary the least active compound **35** was predicted to bind with the selenolotriazine group rotated of about 180°, likely due to the presence of the morpholino substituent avoiding to maintain the same orientation (Supplementary material Figure SM-1D). The 3-D QSAR models predicted these compounds in the range 0.05–1 μ M (Supplementary material Table SM-2), nevertheless these over-predictions are in agreement with the known limitation of the models in which the training set compounds with activities below higher than 1 μ M were not correctly fitted being over-recalculated by the models themselves (Supplementary material Figure SM-2). Overlapping the 3-D QSAR maps to the most active compound **30** indicated that the introduction of further sterical groups into the ATP binding site would have led to more active compounds. Accordingly, a new series of thienopyrimidines/thienotriazines, **1–3** (Fig. 3), were designed and synthesized, in order to better fill the ATP binding site.

The new designed compounds were promptly modeled and subjected to both molecular docking simulation and 3-D QSAR predictions. Most of the new designed molecules were predicted to be in the 0.01–0.1 μ M range (Supplementary material Table SM-3)

and thus, considering the error prediction observed for the above **14**, **30**, **33** and **35** compounds, we expected these molecules to show biological activities in the range on low micromolar or at least submicromolar. Among the analyzed compounds, **2f** was predicted to be in the low nanomolar range. Binding mode exploration of **2f** revealed that indeed the compound occupies the ATP binding site slightly more than **14**, **30**, **33** and **35**, particularly it seems to block more efficiently the ATP pocket (Fig. 5). Furthermore, in Figure SM-3 (Supplementary material) is clearly visible that the thienopyrimidine core of **2f** binds in a reversed way the same region of **14**, **30** and **33** fused-triazine groups and overlaps the **35**-tolyl substituent. In this way, the benzylindole fragment of **2f** fills-up the ATP binding entrance establishing further sterical interactions that could stabilize the **2f**/VEGFR-2 complex (Supplementary material Figure SM-4). In view of this promising scenario, we promptly designed the synthesis of compounds **1–3** to test their biological activities as potential VEGFR-2 inhibitors.

2.2. Chemistry

The synthesis of compounds **1–3** was designed to be achieved by the key intermediate 5-(indol-3-yl)-3-aminothiophene-2-carboxylate or derivatives. Therefore we have developed a multi-step sequence to lead to 5-(indol-3-yl)-3-aminothiophenes **43a–f**

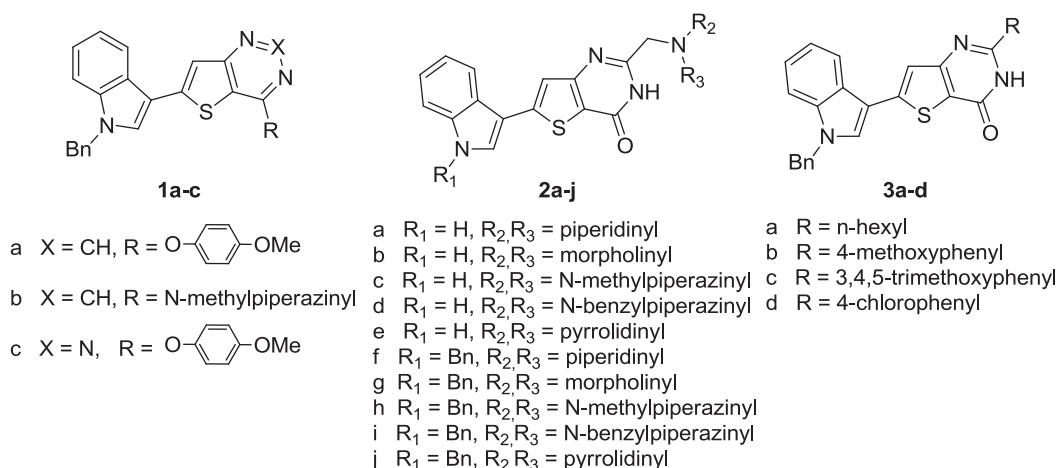
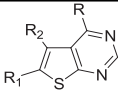


Fig. 3. Designed compounds **1–3**.

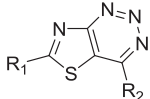
Table 1
Structures and VEGFR-2 inhibitory activities of thieno[3,2-*d*]pyrimidines **4–13**.


#	R	R ₁	R ₂	% Inhibition @ 200 μM ^a
4	4-MeO–C ₆ H ₄	H	H	25.4 ± 2.0
5	4-MeO–C ₆ H ₄	(CH ₂) ₄	H	47.4 ± 1.8
6	3-Ac–C ₆ H ₄	H	H	13.1 ± 0.6
7	3-Ac–C ₆ H ₄	(CH ₂) ₄	H	34.8 ± 2.9
8	3-Indolyl	H	H	23.3 ± 1.6
9	3-Indolyl	(CH ₂) ₄	H	44.9 ± 3.9
10	4-MeO–C ₆ H ₄ O	H	H	64.2 ± 3.8
11	3-Ac–C ₆ H ₄ O	H	H	21.9 ± 1.7
12	3-Ac–C ₆ H ₄ O	(CH ₂) ₄	H	56.9 ± 4.5
13	4-NH ₂ –C ₆ H ₄ O	H	H	40.1 ± 2.4

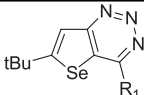
^a Values are means ± SEM of two determinations carried out in triplicate.

(Scheme 1). 5-Aryl-3-aminothiophenes are usually synthesized in our lab starting from acetophenones via β-aryl-β-chloroacroleins, oximes, β-aryl-β-chloroacrylonitriles, condensation with sodium sulfide and activated halogen derivatives and finally by a cyclization step to form the thiophene moiety [39]. However, working on 3-acetylindoles needed to modify the reaction conditions for nearly each step of the synthesis. In particular, 3-acetylindoles **39** were first reacted with Vilsmeier–Haack reagent (formed in situ with phosphorus oxychloride and *N,N*-dimethylformamide) to give β-chloroacroleins. The intermediates iminium salts needed to be trapped and isolated as perchlorates **40**. Iminium salts **40** were then converted to the corresponding oxime **41** [40]. Use of classical conditions for dehydration in β-aryl-β-chloroacrylonitriles (i.e. Ac₂O, PPA, P₂O₅, PCl₅) failed, therefore the expected compounds **42** were obtained in good yields using di-2-pyridinyl thionocarbonate (DPT) [41]. Thiophenes **43** were obtained by treating **42** with ethyl bromoacetate, chloroacetonitrile or chloroacetamide in presence of sodium sulfide followed by cyclization with sodium ethanolate.

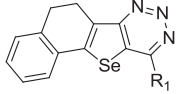
3-Amino-2-cyano-5-indol-3-ylthiophenes **43b** and **43e** were converted into thieno[3,2-*d*]pyrimidin-4-ones **44a** and **44b** in respectively 84% and 88% by action of formic acid in the presence of a catalytic amount of sulfuric acid (Scheme 2) [34]. Then 4-chlorothienopyrimidines **45a** and **45b** were obtained (45% and 98% yields) using phosphorus oxychloride. Finally, compounds **1a** and **1b** were obtained by S_NAr with *p*-methoxyphenolate and *N*-methylpiperazine, respectively. Intermediate **43e** allowed formation of thienotriazine **46** in 88% yield which was then submitted to S_NAr with *p*-methoxyphenolate to give **1c** in 80% yield [37] (Scheme 2).

Table 2
Structures and VEGFR-2 inhibitory activities of thiazolotriazines **14–21**.


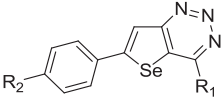
#	R ₁	R ₂	% Inhibition @ 200 μM ^a
14	S–Me	Cl	93.5 ± 7.5
15	NH–Ph	Cl	49.8 ± 2.9
16	NH–Ph	4-Morpholinyl	13.7 ± 1.1
17	1-Pyrrolidinyl	Cl	n.a. ^b
18	1-Pyrrolidinyl	1-Pyrrolidinyl	n.a. ^b
19	1-Pyrrolidinyl	4-Morpholinyl	n.a. ^b
20	4-Morpholinyl	Cl	11.9 ± 0.7
21	4-Morpholinyl	1-Pyrrolidinyl	16.2 ± 1.1

^a Values are means ± SEM of two determinations carried out in triplicate.^b Not active. No inhibition was observed up to 200 μM of the tested compound.**Table 3**
Structures and VEGFR-2 inhibitory activities of selenolotriazines **22–38**.


#	R ₁	R ₂	% Inhibition @ 200 μM ^a
22	1-Pyrrolidinyl	–	n.a. ^b
23	4-Morpholinyl	–	n.a. ^b



24	Cl	–	37.8 ± 3.2
25	1-Pyrrolidinyl	–	17.0 ± 1.0
26	4-Morpholinyl	–	19.4 ± 1.5



27	Cl	H	60.7 ± 4.8
28	1-Pyrrolidinyl	H	20.8 ± 1.4
29	4-Morpholinyl	H	24.7 ± 1.9
30	Cl	Cl	94.6 ± 6.6
31	1-Pyrrolidinyl	Cl	37.8 ± 1.5
32	4-Morpholinyl	Cl	31.0 ± 1.3
33	Cl	CH ₃	88.0 ± 6.1
34	1-Pyrrolidinyl	CH ₃	73.5 ± 6.6
35	4-Morpholinyl	CH ₃	72.5 ± 3.6
36	Cl	OCH ₃	36.5 ± 2.9
37	1-Pyrrolidinyl	OCH ₃	17.6 ± 1.1
38	4-Morpholinyl	OCH ₃	14.8 ± 1.2

^a Values are means ± SEM of two determinations carried out in triplicate.^b Not active. No inhibition was observed up to 200 μM of the test compound.

3-Amino-2-carboxamido-5-indol-3-ylthiophenes **43c** and **43f** were reacted successively with chloroacetyl chloride and a secondary amine to give compounds **48a–j** [42]. Cyclization in thienopyrimidinones **2a–j** was realized in basic media in good yields (Scheme 3). Compounds **2a–j** were converted in hydrochlorides.

Compounds **3a–d** were achieved in moderate yields (12–36%) by condensation reactions between 3-amino-2-carboxamido-5-indol-3-ylthiophene **43f** and the proper aldehydes in the presence of hydrochloric acid (Scheme 4).

2.3. Biological activity of designed compounds **1–3**

The VEGFR-2 inhibitory activities of the newly synthesized compounds **1–3** were evaluated at 200 μM fixed doses (Table 5) and among the sixteen tested derivatives only four (**2b**, **2e**, **2h** and **2j**) were totally inactive. These experimental results are in agreement with the above reported predictions and interestingly the most active predicted compound **2f** was indeed those with the highest

Table 4
IC₅₀ values of selected compounds, **14**, **30**, **33**, **35**. The SB 3-D QSAR predicted pIC₅₀ is also reported in comparison with the experimental pIC₅₀ value.

#	Exp. IC ₅₀ (μM) ^a	Exp. pIC ₅₀	Pred. pIC ₅₀
14	45.2 ± 2.7	4.3	5.9
30	4.1 ± 0.2	5.4	6.0
33	16.7 ± 1.0	4.8	6.0
35	26.2 ± 1.5	4.6	7.1

^a IC₅₀ values represent the concentration required to produce 50% enzyme inhibition. Values ±SEM are the average from at least two independent dose–response curves.

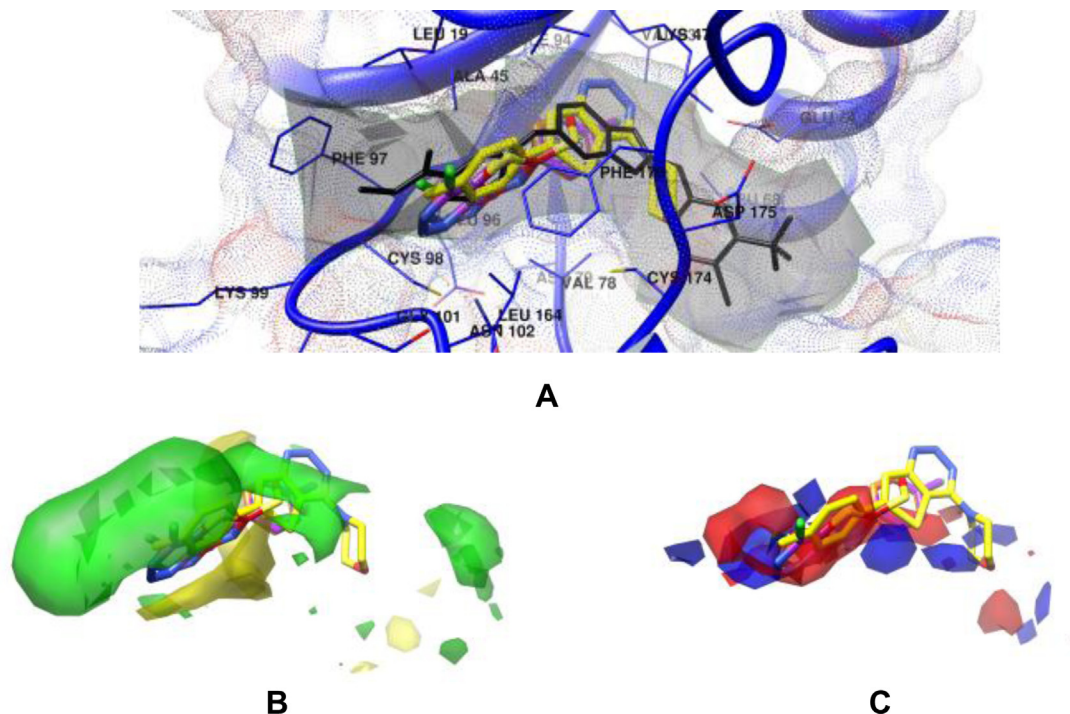


Fig. 4. Docked conformation of **14** (red), **30** (orange), **33** (purple) and **35** (yellow) (A) into VEGFR-2 (PDB ID 2qu5, blue ribbon). As reference the co-crystallized ligand is also displayed in black. The surface of ATP and co-crystallized inhibitor binding site is also shown in light gray. Merged in the steric (B) and electrostatic (C) 3-D QSAR maps. (For interpretation of the references to colour in this figure legend, the reader is referred to the web version of this article.)

percentage of inhibition (99.2%). Both the activity prediction and the fixed dose evaluation were also run on the thiophene intermediates **44b**, **45b** and **48a–j**, but none of those compounds presented higher activity (prediction or experimental result) than the final thienopyrimidine series (Supplementary material Table SM-4).

IC₅₀ values of the most active compounds, **2f** and **3d**, were determined as $2.25 \pm 0.1 \mu\text{M}$ and $15.3 \pm 1.2 \mu\text{M}$, respectively.

To establish further biological activities, endothelial cells were grown in the presence of these molecules. However DMSO, solvent used to dissolve these molecules, was toxic for endothelial cells (Fig. 6). We also noted that the morphology of endothelial cell was affected by DMSO. Their shape was very round when they were incubated with a percentage of DMSO upper to 0.1% whereas they are normally elongated or fusiform. Then, to be

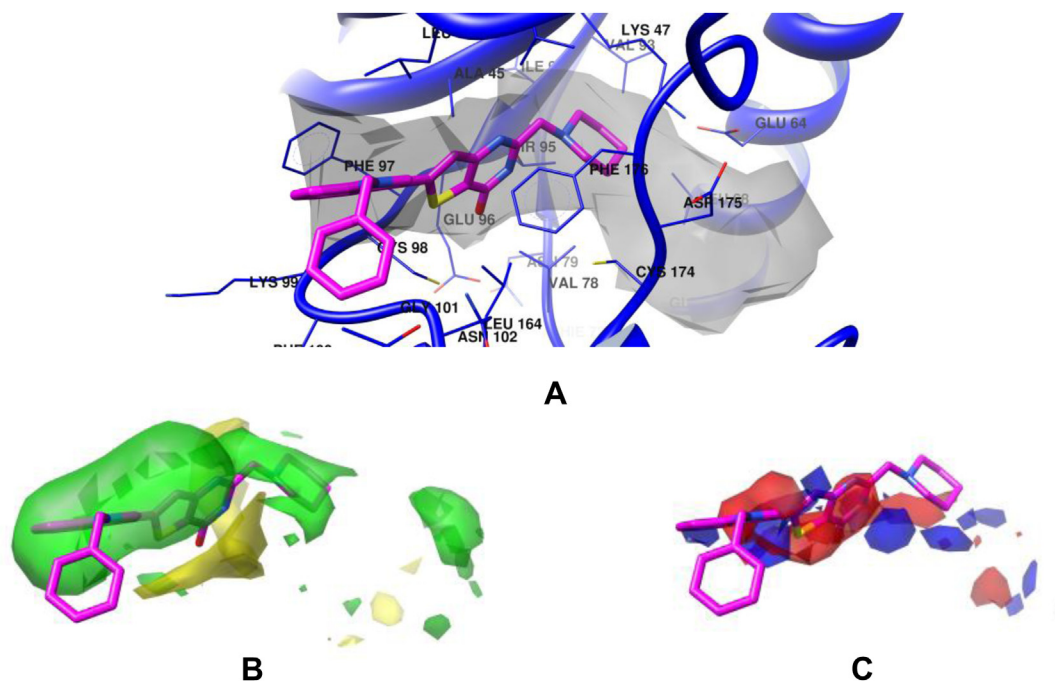
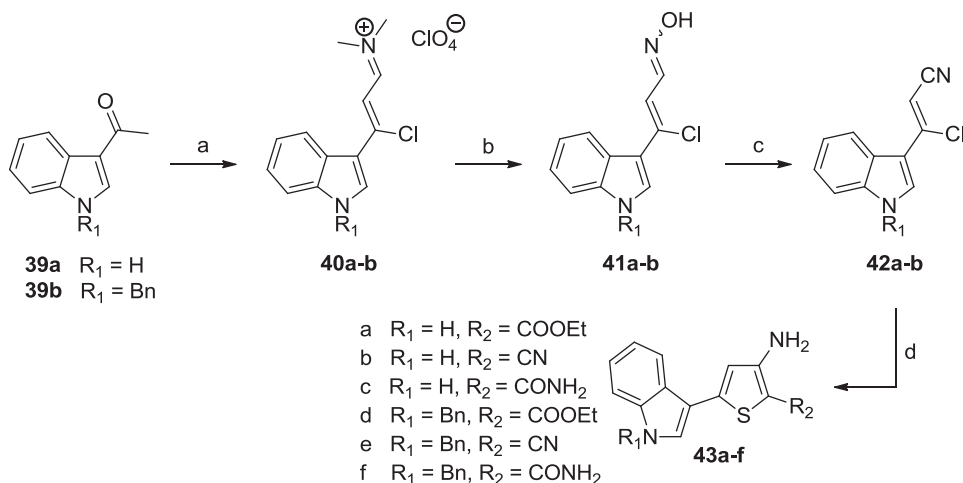


Fig. 5. Docked conformation of **2f** (magenta) (A) into VEGFR-2 (PDB ID 2qu5, blue ribbon). The ATP binding site is also shown in light gray. Merged in the steric (B) and electrostatic (C) 3-D QSAR maps. (For interpretation of the references to colour in this figure legend, the reader is referred to the web version of this article.)



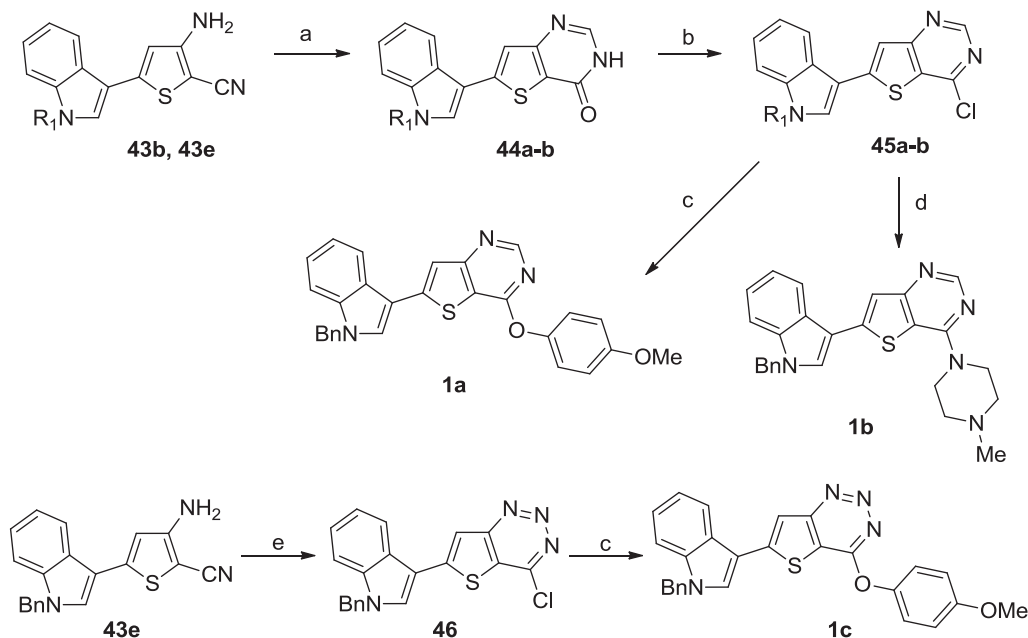
Scheme 1. Synthesis of intermediates **43a–f**. Reagents and conditions: (a) (i) Vilsmeier reagent: $POCl_3/DMF$, $0^\circ C$; $0^\circ C$ to RT. (ii) $NaClO_4$, H_2O . (b) $NH_2OH.HCl$, $CH_3COONa.3H_2O$, $EtOH$. (c) Di-2-pyridyl thionocarbonate, DMAP, CH_2Cl_2 . (d) (i) $Na_2S.9H_2O$. (ii) $X-CH_2-R_2$. (iii) $EtONa$ DMF, $50^\circ C$.

able to investigate the activity of those molecules, it was required to work with less than 0.1% DMSO in culture media supplemented with 2% SVF. As a matter of fact most of the newly prepared derivatives were poorly soluble in biological media containing 0.1% DMSO with precipitate formation upon dilution at physiological pH. Therefore we focused on derivative **2f** by preparing a series of salts (hydrochloride, methylsulfonate, phosphate and tartaric acid), among them only **2f** tartaric acid salt (**2f·tartaric**) showed the needed solubility in biological media to test its activity on our cellular model.

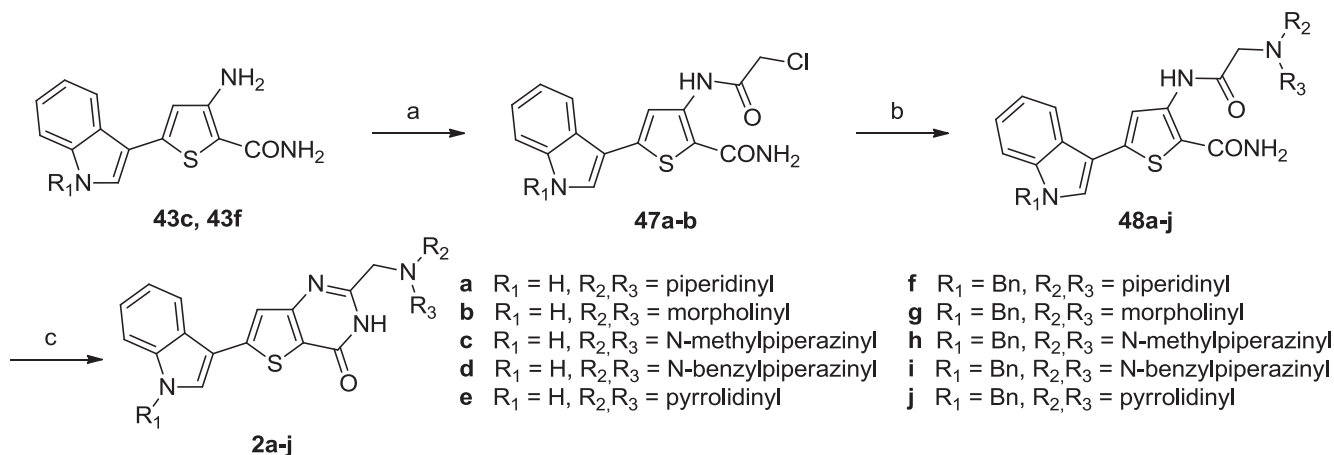
Study of the biological effect of **2f·tartaric** consists at the first step to the analysis of its effect on metabolic activity and viability of endothelial cells and at the second step to the analysis of the angiogenic activity of these cells.

Metabolic activity of HUVEC decreased with **2f·tartaric** concentration (-9% at $1.5 \mu M$ until -51% at $100 \mu M$) (Fig. 7) in a dose dependant manner (EC_{50} was estimated at about $12 \mu M$). In contrary, no variation in HUVEC viability was induced by **2f·tartaric** whatever the concentration used (Fig. 7). These results suggest that this compound had a cytostatic rather than cytotoxic activity on endothelial cells.

To further investigate the angiogenic activity of **2f·tartaric**, we used our *in vitro* model of endothelial cell tube formation in which HUVEC were plated onto matrigel®-coated well and cultured with or without **2f·tartaric** in the presence of VEGF during 24 h and using Sunitinib as anti-VEGFR-2 reference. As we can see in Fig. 8, VEGF alone (positive control) induced endothelial cell tube formation of HUVEC as compared with control medium without VEGF



Scheme 2. Synthesis of derivatives **1a–c**. Reagents and conditions: (a) $HCOOH$, H_2SO_4 , $40^\circ C$. (b) $POCl_3/DMF$, $0^\circ C$ to r.t. (c) $MeOC_6H_4ONa$, DMF, r.t. (d) *N*-Methylpiperazine, DMF, r.t. (e) $NaNO_2$, HCl 37%, $0^\circ C$ to r.t.



Scheme 3. Synthesis of derivatives **2a–j**. Reagents and conditions: (a) Chloroacetyl chloride, Et_3N , THF, 0°C to r.t. (b) $\text{R}_2\text{R}_3\text{NH}$, K_2CO_3 , CH_3CN , reflux. (c) NaOH 2N, DMF, reflux.

(negative control). This was correlated with the decrease of area fraction found after VEGF exposure. Angiogenesis induced by VEGF was completely inhibited using $1\ \mu\text{M}$ of **2f-tartaric** and $3\ \mu\text{M}$ of Sunitinib (upper part of Fig. 8). **2f-tartaric** can inhibit endothelial cell tube formation induced by VEGF in a dose dependent manner showing an estimated EC_{50} value of about 31 nM. Using the same model for Sunitinib the EC_{50} resulted to be 645 nM. The number of contiguous cells was increased whereas the number of endothelial cell tubes was decreased and area fraction was equivalent to that of control media without VEGF (Fig. 8).

3. Conclusion

In this paper we present a multidisciplinary approach to the design, synthesis and biological characterization of thienopyrimidines as new class of VEGFR-2 inhibitors. The new compounds **1–3** were designed starting from a small fragment library (**4–38**) on which biological evaluation and SB 3-D QSAR studies were conducted in parallel. The modeling approach proved to be an effective tool to predict the activity of the preliminary series of compounds. Binding mode analysis of the most active derivatives (**14**, **30**, **33** and **35**) led to the design of a new series of thienopyrimidines (**1–3**) that were prepared by a multi-step synthetic pathway ad-hoc designed. Among the newly synthesized, compound **2f**, showed the highest activity, as predicted by the 3-D QSAR approach. Further biological assays on endothelial cell tube formation proved **2f** as a new anti-angiogenic lead compound that showed to be more efficient in inhibiting endothelial cell tube formation induced by VEGF compared with Sunitinib, in our *in vitro* model. Moreover **2f** did not cause any cytotoxic side effect to endothelial cells.

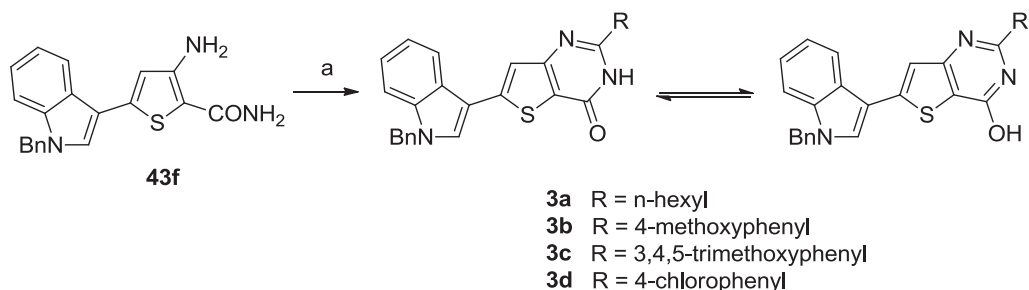
We have tested the specificity of **2f** for the inhibition of activated RTK in HUVEC using Human Phospho-RTK Proteome profiler array kit (RetD system, United Kingdom) and found that, as Sunitinib, **2f** decreased the phosphorylation of VEGFR-1 and VEGFR-2 (data not shown). Furthermore we found that **2f** decrease also the phosphorylation of others RTK activated in HUVEC such as EGFR, Axl, Dtk, ROR-2, Tie-1 and EphA6, receptors implicated in the development of cancer (Supplementary material Figure SM-5).

The binding mode of **2f** suggests that a further substitution on piperidine positions 3 and 4 would lead to better ATP binding pocket filling and, eventually, to more active derivatives (Fig. 9). To this aim a focused virtual screening on **2f** derivatives is currently ongoing and further synthetic efforts will be based on binding mode evaluation and 3-D QSAR predictions.

4. Experimental section

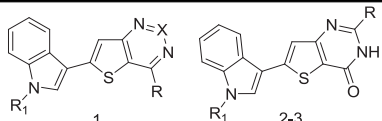
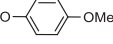
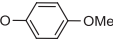
4.1. Chemistry

All starting materials and synthesis reagents were obtained commercially. Column chromatography was performed with silica gel 60 (particle size 70–200 μm). Thin-layer chromatography (TLC) was performed on Merck pre-coated TLC aluminum sheets with silica gel 60 F254. Melting points were determined on a Stuart SMP3 apparatus and are uncorrected. ^1H NMR spectra were measured at 250 MHz, and ^{13}C NMR spectra were measured at 62.5 MHz on a Bruker Advance AC 250 spectrometer at 25°C in CDCl_3 , $\text{DMSO}-d_6$ or $\text{acetone}-d_6$, and chemical shifts are given in ppm (δ). The spectral splitting patterns are designated as follows: s, singlet; d, doublet; t, triplet; q, quartet; m, multiplet; br s, broad singlet. Representative ^1H and ^{13}C NMR spectra for **1a**, **2f**, **2g** and **2i**



Scheme 4. Synthesis of derivatives **3a–d**. Reagents and conditions: (a) RCHO , MeOH, 6% HCl (w/w).

Table 5
Structures and VEGFR-2 inhibitory activities of 5-indolylthienopyrimidine/triazines **1** and 5-indolylthieno[3,2-*d*]pyrimidinones **2–3**.

				
#	X	R	R ₁	% Inhibition @ 200 μM ^a
1a	CH		Benzyl	38.8 ± 3.5
1b	CH	N-Methylpiperazinyl	Benzyl	n.t. ^b
1c	N		Benzyl	1.7 ± 0.1
2a	–	1-Piperidinylmethyl	H	5.7 ± 0.4
2b	–	1-Morpholinylmethyl	H	n.a. ^c
2c	–	1-(4-Methylpiperazinyl)methyl	H	3.9 ± 0.2
2d	–	1-(4-Benzylpiperazinyl)methyl	H	2.1 ± 0.1
2e	–	1-Pyrrolidinylmethyl	H	n.a. ^c
2f	–	1-Piperidinylmethyl	Benzyl	99.2 ± 3.9
2g	–	1-Morpholinylmethyl	Benzyl	52.6 ± 3.7
2h	–	1-(4-Methylpiperazinyl)methyl	Benzyl	n.a. ^c
2i	–	1-(4-Benzylpiperazinyl)methyl	Benzyl	19.0 ± 0.7
2j	–	1-Pyrrolidinylmethyl	Benzyl	n.a. ^c
3a	–	Hexyl	Benzyl	35.2 ± 2.8
3b	–	4-Methoxyphenyl	Benzyl	40.9 ± 2.8
3c	–	3,4,5-Trimethoxyphenyl	Benzyl	52.0 ± 3.6
3d	–	4-Chlorophenyl	Benzyl	73.4 ± 6.5

^a Values are means ± SEM of two determinations carried out in triplicate.

^b Not tested.

^c Not active. No inhibition was observed up to 200 μM of the test compound.

are reported in [Supplementary material Figures SM-7–SM-13](#). IR spectra were recorded for neat samples on KBr plates on a Perkin Elmer Spectrum Bx FTIR spectrophotometer or on a Perkin Elmer FTIR Baragon 1000PC equipped with a Graseby-Specac golden gate. HRMS were collected on a Bruker MICROTOF-Q ESI/QqTOF spectrometer. Elemental analyses (C, H, N, S) were used to confirm the purity of all tested compounds (>95%) and were performed on a CHN ThermoScientific Flash 2000 apparatus.

4.1.1. N-Benzyl-3-acetylindole (**39b**)

To a solution of 3-acetylindole (382 mg, 2.40 mmol) in ethanol (20 mL) was added potassium hydroxide (168 mg, 3 mmol) and the reaction mixture was stirred at room temperature until dissolution. The solvent was removed under reduced pressure and dry acetone

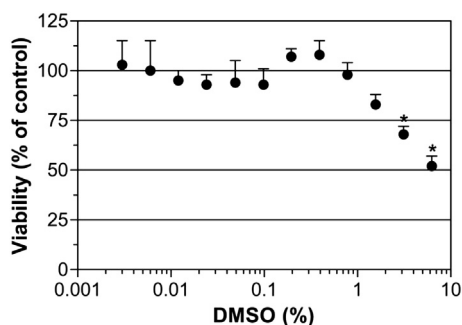


Fig. 6. Effect of DMSO on the viability of endothelial cells. Viability of HUVEC (black circle) was measured after 24 h of exposure of HUVEC to DMSO (0–6% v/v) in culture media containing 2% SVF. Results are presented as relative values to untreated cells ($n = 3$, triplicate). Differences are considered as significant when $p < 0.05$ using Bonferroni/Dunn test. *Versus control medium without DMSO.

was added followed by benzyl bromide (0.29 mL, 2.40 mmol). After 5 min, solid was filtered and filtrate was dried under reduced pressure to afford a white solid (586 mg, 2.35 mmol, 98%); mp 114 °C (Lit. [43]: 114–115 °C); ¹H NMR (250 MHz, DMSO-*d*₆) δ (ppm): 2.45 (s, 3H, CH₃), 5.49 (s, 2H, CH₂), 7.17–7.20 (m, 2H, 2× CH), 7.17–7.33 (m, 5H, 5× CH), 7.49–7.53 (m, 1H, CH), 8.16–8.20 (m, 1H, CH), 8.53 (s, 1H, CH). ¹³C NMR (62.5 MHz, DMSO-*d*₆) δ (ppm): 27.3, 49.7, 111.0, 116.1, 121.6, 122.0, 122.9, 125.9, 127.2, 127.6, 128.6, 136.5, 137.0, 137.4, 192.3.

4.1.2. [3-Chloro-3-(indol-3-(1H)-yl)prop-2-enylidene]dimethyliminium perchlorate (**40a**)

To a solution of phosphorus oxychloride (27.96 mL, 300 mmol) was added dropwise dry DMF (23.20 mL, 300 mmol) at 0 °C. Then, the solution was stirred until formation of Vilsmeier–Haack reagent. After 30 min, 3-acetylindole (15.92 g, 100 mmol) dissolved in DMF (120 mL) was added dropwise. An orange solid appeared instantly. The solution was stirred at room temperature until dissolution of precipitated and after 2 h a pale orange solid formed in suspension of DMF. After 1 h, the reaction mixture was poured with good stirring into ice-water (800 mL) containing sodium perchlorate (24.49 g, 200 mmol). The precipitate was filtered and washed with Et₂O. The solid was purified in CHCl₃, filtered while hot to afford an orange solid (>95%, hygroscopic); mp 251 °C (Lit. [44]: 246–248 °C); ¹H NMR (250 MHz, DMSO-*d*₆) δ (ppm): 3.55 (s, 3H, CH₃), 3.65 (s, 3H, CH₃), 7.13 (d, 1H, CH, $J = 10.5$ Hz), 7.31–7.40 (m, 2H, 2× CH), 7.56–7.61 (m, 1H, CH), 8.09–8.14 (m, 1H, CH), 8.60 (d, 1H, CH, $J = 3.4$ Hz), 8.79 (d, 1H, CH, $J = 10.5$ Hz), 12.87 (br s, 1H, NH). ¹³C NMR (62.5 MHz, DMSO-*d*₆) δ (ppm): 41.2, 48.4, 107.1, 113.6, 114.2, 121.0, 123.8, 124.2, 125.0, 137.2, 138.1, 153.5, 163.3. HRMS (ESI): m/z calcd for C₁₃H₁₄ClN₂: 233.0840; found: 233.0835.

4.1.3. [3-Chloro-3-(1-benzyl-1H-indol-3-yl)prop-2-enylidene]dimethyliminium perchlorate (**40b**)

The same procedure as for **40a** was used and afforded an orange solid (>95%, hygroscopic); mp 168 °C; ¹H NMR (250 MHz, DMSO-*d*₆) δ (ppm): 3.51 (s, 3H, CH₃), 3.67 (s, 3H, CH₃), 5.61 (s, 2H, CH₂), 7.15 (d, 1H, CH, $J = 10.5$ Hz), 7.26–7.40 (m, 8H, 8× CH), 7.67–7.70 (m, 1H, CH), 8.13–8.17 (m, 1H, CH), 8.84 (s, 1H, CH). ¹³C NMR (62.5 MHz, DMSO-*d*₆) δ (ppm): 41.2, 48.5, 50.2, 107.7, 112.6, 113.6, 121.3, 123.6, 124.4, 127.3, 128.0, 128.7, 136.1, 137.8, 139.5, 152.5, 163.4. HRMS (ESI): m/z calcd for C₂₀H₂₀ClN₂: 323.1310; found: 323.1310.

4.1.4. 3-Chloro-3-(1H-indol-3-yl)-2-propenal oxime (**41a**)

To a solution of [3-chloro-3-(indol-3-(1H)-yl)prop-2-enylidene]dimethylammonium perchlorate **40a** (33.32 g, 100 mmol) in ethanol (150 mL) were added hydroxylamine hydrochloride (10.42 g, 150 mmol) followed by sodium acetate trihydrate (13.61 g, 100 mmol). The reaction mixture was heated at 60 °C for 6 h and kept at room temperature overnight. The solution was poured into ice-water, filtered and washed with cold water. The solid was triturated in CH₂Cl₂ to give a beige solid (17.87 g, 81 mmol, 81%); mp 99 °C; IR (neat): 3118 (OH), 3354 (NH) cm^{–1}; ¹H NMR (250 MHz, DMSO-*d*₆) δ (ppm): 6.84 + 7.33 (d + d, 1H, CH, $J = 9.4$ Hz), 7.12–7.23 (m, 2H, 2× CH), 7.47 (d, 1H, CH, $J = 9.4$ Hz), 7.61 + 8.16 (d + d, 1H, CH, $J = 9.4$ Hz), 7.75–7.87 (m, 2H, 2× CH), 11.32 + 11.51 (s + s, 1H, OH), 11.74 + 11.84 (br s + br s, 1H, NH). ¹³C NMR (62.5 MHz, DMSO-*d*₆) δ (ppm): 20.6, 98.4, 117.2, 124.6, 129.5, 129.6, 131.2, 136.7, 141.8, 145.6, 161.6. HRMS (APCI): m/z calcd for C₁₁H₁₀ClN₂O: 221.0476; found: 221.0487.

4.1.5. 3-(1-Benzyl-1H-indol-3-yl)-3-chloro-2-propenal oxime (**41b**)

This compound was synthesized using the same procedure as for **41a** starting with [3-chloro-3-(1-benzyl-1H-indol-3-yl)prop-2-enylidene]dimethylammonium perchlorate **40b** to afford a pale

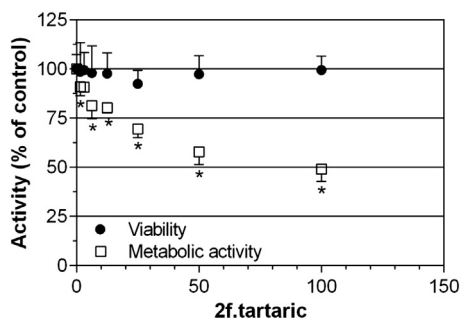


Fig. 7. Effect of **2f-tartaric** on metabolic activity and viability of endothelial cells. Metabolic activity (open square) and viability (black circle) were measured after 24 h of exposure of HUVEC to **2f-tartaric** (0–100 μM). Results are presented as relative values to untreated cells ($n = 3$, triplicate). Differences are considered as significant when $p < 0.05$ using Bonferroni/Dunn test. *Versus control medium without **2f-tartaric**.

yellow solid (20.82 g, 67 mmol, 67%); mp 69 °C; IR (neat): 3168 (OH) cm^{-1} ; ^1H NMR (250 MHz, $\text{DMSO-}d_6$) δ (ppm): 5.47 + 5.49 (s + s, 2H, CH_2), 6.87 + 7.36 (d + d, 1H, CH, $J = 9.4$ Hz), 7.17–7.31 (m, 7H, 7 × CH), 7.52–7.58 (m, 1H, CH), 7.62–8.17 (d + d, 1H, CH, $J = 9.4$ Hz), 7.78–7.88 (m, 1H, CH), 8.06 + 8.13 (s + s, 1H, CH), 11.36 + 11.55 (s + s, 1H, OH). ^{13}C NMR (62.5 MHz, $\text{DMSO-}d_6$) δ (ppm): 49.28, 49.34, 108.4, 111.4, 111.6, 112.86, 112.88, 115.4, 119.5, 119.8, 121.2, 121.5, 122.7, 122.8, 124.08, 124.14, 127.1, 127.2, 127.5, 127.6, 128.60, 128.62, 131.0, 131.4, 132.6, 132.9, 136.9, 137.0, 137.2, 137.3, 143.0, 146.9. HRMS (ESI): m/z calcd for $\text{C}_{18}\text{H}_{16}\text{ClN}_2\text{O}$: 311.0946; found: 311.0945.

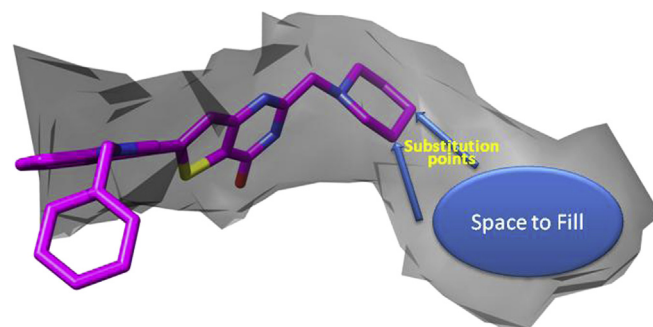


Fig. 9. Model for the molecules to be designed. In shaded gray is represented the ATP binding site. The two arrows indicate possible point for substitution on the **2f** piperidine ring. The new molecules will be designed to fill the blue oval. (For interpretation of the references to colour in this figure legend, the reader is referred to the web version of this article.)

4.1.6. 3-Chloro-3-(1H-indol-3-yl)-2-propenenitrile (**42a**)

To a solution of 3-chloro-3-(1H-indol-3-yl)-2-propenal oxime (**41a**) (3.00 g, 13.60 mmol) in CH_2Cl_2 (60 mL) were added di-2-pyridyl thionocarbonate (3.16 g, 13.60 mmol) followed by 4-*N*,*N*-dimethylaminopyridine (249 mg, 2.04 mmol). The solution was stirred overnight at room temperature. The reaction mixture was filtered on Celite and the filtrate was washed once with HCl 3% (30 mL) and once with NaHCO_3 10% (30 mL), dried on MgSO_4 and concentrated under reduce pressure. The residue was purified by silica gel column chromatography (cyclohexane:AcOEt = 80:20) to provide an orange solid (2.45 g, 12 mmol, 89%); mp 102 °C; IR (KBr): 2209 (CN) cm^{-1} ; ^1H NMR (250 MHz, $\text{DMSO-}d_6$) δ (ppm): 6.45 (s, 1H,

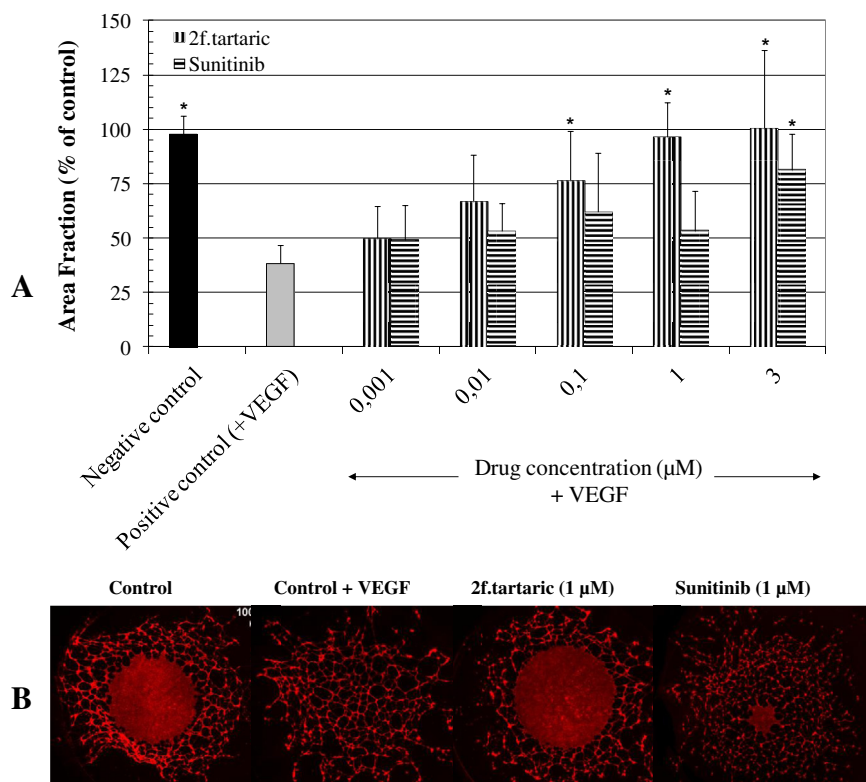


Fig. 8. Effect of **2f-tartaric** on endothelial cell tube formation. HUVEC were plated onto matrigel[®]-coated well and cultured in control media with 50 ng VEGF, **2f-tartaric** and Sunitinib as positive control. (A) Area fraction of endothelial cells was measured using NIS Element software and presented as percentage of variation with values obtained for control medium without VEGF as reference (negative control) ($n = 5$). Differences are considered as significant when $p < 0.05$ using PLSD Fisher statistical test. *Versus positive control medium without **2f-tartaric** (control + VEGF). (B) Photomicrographs were taken after fixation and phalloidin-sulfo-rhodamine staining and are representative of 5 experiments. Area fraction was calculated as area of cells in relation to whole field. Scale bar represent 1000 μm.

CH), 7.18–7.29 (m, 2H, 2× CH), 7.48–7.53 (m, 1H, CH), 7.92–7.97 (m, 1H, CH), 8.05 (s, 1H, CH), 12.18 (br s, 1H, NH). ^{13}C NMR (62.5 MHz, DMSO- d_6) δ (ppm): 89.8, 111.6, 112.9, 117.4, 119.8, 121.8, 123.1, 123.2, 132.0, 137.4, 145.6. HRMS (APCI): m/z calcd for $\text{C}_{11}\text{H}_8\text{ClN}_2$: 203.0371; found: 203.0373.

4.1.7. 3-(1-Benzyl-1H-indol-3-yl)-3-chloro-2-propenenitrile (**42b**)

This compound was synthesized using the same procedure as for **42a** starting with 3-(1-benzyl-1H-indol-3-yl)-3-chloro-2-propenal oxime **41b**. The residue was purified by silica gel column chromatography (cyclohexane:AcOEt = 80:20) to afford a beige solid (3.46 g, 11.83 mmol, 87%); mp 124 °C; IR (KBr): 2208 (CN) cm^{-1} ; ^1H NMR (250 MHz, DMSO- d_6) δ (ppm): 5.52 (s, 2H, CH_2), 6.48 (s, 1H, CH), 7.20–7.34 (m, 7H, 7× CH), 7.56–7.60 (m, 1H, CH), 7.95–7.99 (m, 1H, CH), 8.31 (s, 1H, CH). ^{13}C NMR (62.5 MHz, DMSO- d_6) δ (ppm): 49.5, 90.4, 111.2, 111.8, 117.3, 120.1, 122.2, 123.3, 123.8, 127.2, 127.7, 128.7, 135.0, 136.8, 137.2, 145.0. HRMS (APCI): m/z calcd for $\text{C}_{18}\text{H}_{14}\text{ClN}_2$: 293.0840; found: 293.0839.

4.1.8. Ethyl 3-amino-5-(1H-indol-3-yl)-2-thiophenecarboxylate (**43a**)

A suspension of sodium sulfide nonahydrate (2.40 g, 10 mmol) in DMF (15 mL) was heated at 40 °C for 30 min. 3-Chloro-propenenitrile (2.03 g, 10 mmol) dissolved in DMF (15 mL) was added dropwise and the solution was heated at 50 °C for 2 h. Then, ethyl bromoacetate (1.11 mL, 10 mmol) in DMF (5 mL) was added dropwise and the reaction mixture was stirred at 50 °C for 2 h. A solution of NaOEt (681 mg, 10 mmol) in absolute ethanol was added and the solution was stirred at 50 °C for 2 h (the reaction was monitored by TLC). The reaction mixture was then cooled to room temperature, diluted with water (200 mL) and extracted three times with AcOEt (25 mL). The organic layer was dried over anhydrous magnesium sulfate and the solvent was evaporated under reduce pressure. The residue was purified by silica gel column chromatography (cyclohexane:AcOEt = 50:50) to provide a yellow oil (344 mg, 1.20 mmol, 12%); ^1H NMR (250 MHz, CDCl_3) δ (ppm): 1.29 (t, 3H, CH_3 , $J = 7.18$ Hz), 4.24 (q, 2H, CH_2 , $J = 7.10$ Hz), 5.09 (br s, 2H, NH_2), 6.64 (br s, 1H, CH), 7.11–7.21 (m, 2H, 2× CH), 7.28–7.33 (m, 1H, CH), 7.37–7.38 (m, 1H, CH), 7.87–7.91 (m, 1H, CH), 8.49 (br s, 1H, NH). ^{13}C NMR (62.5 MHz, CDCl_3) δ (ppm): 14.7, 60.0, 98.3, 111.3, 111.7, 114.4, 120.0, 121.1, 123.0, 123.3, 124.9, 136.5, 143.8, 154.4, 164.9. HRMS (ESI): m/z calcd for $\text{C}_{15}\text{H}_{14}\text{N}_2\text{O}_2\text{SNa}$: 309.0668; found: 309.0661.

4.1.9. 3-Amino-5-(1H-indol-3-yl)-2-thiophenecarbonitrile (**43b**)

This compound was synthesized using the same procedure as for **43a** starting with 3-chloro-3-(1H-indol-3-yl)-2-propenenitrile **42a** and chloroacetonitrile. After cooling, the reaction mixture was poured into ice-water (200 mL) and the precipitate was filtered and washed with cold water. The residue was purified by silica gel column chromatography (cyclohexane:AcOEt = 70:30) to provide a beige solid (383 mg, 1.6 mmol, 16%); mp 138 °C; IR (neat): 2184 (CN), 3372, 3399 (NH_2) cm^{-1} ; ^1H NMR (250 MHz, DMSO- d_6) δ (ppm): 6.42 (br s, 2H, NH_2), 6.83 (s, 1H, CH), 7.13–7.22 (m, 2H, 2× CH), 7.44–7.48 (m, 1H, CH), 7.76–7.80 (m, 1H, CH), 7.85–7.86 (m, 1H, CH), 11.66 (br s, 1H, NH). ^{13}C NMR (62.5 MHz, DMSO- d_6) δ (ppm): 71.4, 108.6, 112.4, 113.2, 116.4, 118.8, 120.5, 122.2, 124.1, 125.3, 136.6, 143.7, 157.8. HRMS (ESI): m/z calcd for $\text{C}_{13}\text{H}_9\text{N}_3\text{SNa}$: 262.0409; found: 262.0416.

4.1.10. 3-Amino-5-(1H-indol-3-yl)-2-thiophenecarboxamide (**43c**)

This compound was synthesized using the same procedure as for **43a** starting with 3-chloro-3-(1H-indol-3-yl)-2-propenenitrile **42a** and chloroacetamide diluted in DMF (5 mL). After cooling, the reaction mixture was poured into ice-water (200 mL) and the precipitate was filtered and washed with cold water. The solid was

trituated in Et_2O and filtered to afford a brown solid (1.78 g, 6.9 mmol, 69%); mp 196 °C; IR (KBr): 1632, 2203, 3177 (CONH_2), 3305, 3441 (NH_2) cm^{-1} . ^1H NMR (250 MHz, DMSO- d_6) δ (ppm): 6.46 (br s, 2H, NH_2), 6.57 (br s, 2H, NH_2), 6.82 (s, 1H, CH), 7.10–7.21 (m, 2H, 2× CH), 7.43–7.47 (m, 1H, CH), 7.75 (m, 1H, CH), 7.84–7.87 (m, 1H, CH), 11.53 (sl, 1H, NH). ^{13}C NMR (62.5 MHz, DMSO- d_6) δ (ppm): 97.5, 109.4, 112.2, 114.5, 119.0, 120.1, 121.9, 124.2, 124.4, 136.6, 139.2, 153.8, 166.4. HRMS (ESI): m/z calcd for $\text{C}_{13}\text{H}_{12}\text{N}_3\text{OS}$: 258.0696; found: 258.0676.

4.1.11. Ethyl 3-amino-5-(1-benzyl-1H-indol-3-yl)-2-thiophenecarboxylate (**43d**)

This compound was synthesized using the same procedure as for **43a** starting with 3-(1-benzyl-1H-indol-3-yl)-3-chloro-2-propenenitrile **42b**. The residue was purified by silica gel column chromatography (cyclohexane:AcOEt = 70:30) to afford a pale yellow solid (2.26 g, 6 mmol, 60%); mp 139 °C; IR (KBr): 1646 (CO), 3352, 3458 (NH_2) cm^{-1} ; ^1H NMR (250 MHz, DMSO- d_6) δ (ppm): 1.26 (t, 3H, CH_3 , $J = 7.05$ Hz), 4.19 (q, 2H, CH_2 , $J = 7.05$ Hz), 5.46 (s, 2H, CH_2), 6.54 (br s, 2H, NH_2), 6.88 (s, 1H, CH), 7.17–7.24 (m, 2H, 2× CH), 7.28–7.34 (m, 5H, 5× CH), 7.53–7.57 (m, 1H, CH), 7.83–7.86 (m, 1H, CH), 8.09 (s, 1H, CH). ^{13}C NMR (62.5 MHz, DMSO- d_6) δ (ppm): 14.5, 49.3, 59.1, 93.8, 108.9, 111.1, 113.8, 119.4, 120.8, 122.3, 124.9, 127.2, 127.5, 128.4, 128.6, 136.3, 137.5, 142.6, 155.6, 163.6. HRMS (ESI): m/z calcd for $\text{C}_{22}\text{H}_{20}\text{N}_2\text{O}_2\text{SNa}$: 399.1138; found: 399.1137.

4.1.12. 3-Amino-5-(1-benzyl-1H-indol-3-yl)-2-thiophenecarbonitrile (**43e**)

This compound was synthesized using the same procedure as for **43a** starting with 3-(1-benzyl-1H-indol-3-yl)-3-chloro-2-propenenitrile **42b** and chloroacetonitrile. After cooling, the reaction mixture was poured into ice-water (200 mL) and the precipitate was filtered and washed with cold water. The solid was trituated in petroleum ether and filtered to afford a pale yellow solid (3.20 g, 9.7 mmol, 97%); mp 160 °C; IR (KBr): 2186 (CN), 3380, 3479 (NH_2) cm^{-1} ; ^1H NMR (250 MHz, DMSO- d_6) δ (ppm): 5.46 (s, 2H, CH_2), 6.47 (br s, 2H, NH_2), 6.84 (s, 1H, CH), 7.16–7.22 (m, 2H, 2× CH), 7.24–7.34 (m, 5H, 5× CH), 7.53–7.57 (m, 1H, CH), 7.78–7.82 (m, 1H, CH), 8.09 (s, 1H, CH). ^{13}C NMR (62.5 MHz, DMSO- d_6) δ (ppm): 49.3, 71.5, 108.3, 111.2, 113.5, 116.3, 119.1, 120.9, 122.5, 124.7, 127.2, 127.5, 128.6, 136.3, 137.4, 143.0, 157.8, 157.9. HRMS (ESI): m/z calcd for $\text{C}_{20}\text{H}_{15}\text{N}_3\text{SNa}$: 352.0879; found: 352.0879.

4.1.13. 3-Amino-5-(1-benzyl-1H-indol-3-yl)-2-thiophenecarboxamide (**43f**)

This compound was synthesized using the same procedure as for **43a** starting with 3-(1-Benzyl-1H-indol-3-yl)-3-chloro-2-propenenitrile **42b** and chloroacetamide diluted in DMF (5 mL). After cooling, the reaction mixture was poured into ice-water (200 mL) and the precipitate was filtered and washed with cold water. The residue was purified by silica gel column chromatography (cyclohexane:AcOEt = 50:50) to provide a pale brown solid (2.47 g, 7.1 mmol, 70%); mp 178 °C; IR (KBr): 1655, 2361, 3137 (CONH_2), 3314, 3455 (NH_2) cm^{-1} . ^1H NMR (250 MHz, DMSO- d_6) δ (ppm): 5.46 (s, 2H, CH_2), 6.47 (br s, 2H, NH_2), 6.76 (br s, 2H, NH_2), 6.82 (s, 1H, CH), 7.16–7.20 (m, 2H, 2× CH), 7.22–7.33 (m, 5H, 5× CH), 7.52–7.56 (m, 1H, CH), 7.85–7.89 (m, 1H, CH), 7.95 (s, 1H, CH). ^{13}C NMR (62.5 MHz, DMSO- d_6) δ (ppm): 49.2, 97.6, 109.2, 111.0, 114.8, 119.4, 120.5, 122.2, 125.0, 127.2, 127.5, 127.6, 128.6, 136.3, 137.6, 138.5, 153.9, 166.3. HRMS (ESI): m/z calcd for $\text{C}_{20}\text{H}_{17}\text{N}_3\text{OSNa}$: 370.0985; found: 370.0983.

4.1.14. 6-(1H-Indol-3-yl)thieno[3,2-d]pyrimidin-4(3H)-one (**44a**)

In round-bottom flask was introduced formic acid (10 mL) and the solution was put at 0 °C. 3-Amino-5-(1H-indol-3-yl)-2-

thiophenecarbonitrile **43b** (239 mg, 1 mmol) was added slowly followed by 30 drops of concentrated sulfuric acid. After 30 min, the ice bath was removed and the reaction was heated at 40 °C for 24 h. The reaction mixture was then cooled to room temperature and poured into ice-water (50 mL). The precipitate was filtered, washed twice with water and once with Et₂O to afford a brown solid (225 mg, 0.84 mmol, 84%); mp 162 °C; IR (neat): 1637 (C=O), 3215 (NH) cm⁻¹. ¹H NMR (250 MHz, DMSO-*d*₆) δ (ppm): 7.19–7.23 (m, 2H, 2× CH), 7.47–7.51 (m, 1H, CH), 7.59 (s, 1H, CH), 7.95–7.99 (m, 1H, CH), 8.08–8.09 (m, 1H, CH), 8.13 (s, 1H, CH), 11.79 (br s, 1H, NH), 12.37 (br s, 1H, NH). ¹³C NMR (62.5 MHz, DMSO-*d*₆) δ (ppm): 114.3, 117.6, 122.9, 124.1, 124.3, 126.0, 127.5, 129.4, 131.3, 142.0, 151.7, 152.0, 162.0, 163.9. HRMS (ESI): *m/z* calcd for C₁₄H₉N₃OSNa: 290.0359; found: 290.0369.

4.1.15. 6-(1-Benzyl-1H-indol-3-yl)thieno[3,2-*d*]pyrimidin-4(3H)-one (**44b**)

This compound was synthesized using the same procedure as for **44a** starting with 3-amino-5-(1-benzyl-1H-indol-3-yl)-2-thiophene carbonitrile **43e** to provide a beige solid (315 mg, 0.88 mmol, 88%); mp 286 °C; IR (KBr): 1659 (C=O), 2789 (NH) cm⁻¹. ¹H NMR (250 MHz, DMSO-*d*₆) δ (ppm): 5.50 (s, 2H, CH₂), 7.18–7.36 (m, 7H, 7× CH), 7.54–7.59 (m, 1H, CH), 7.61 (s, 1H, CH), 7.97–8.04 (m, 1H, CH), 8.14 (s, 1H, CH), 8.30 (s, 1H, CH), 12.41 (br s, 1H, NH). ¹³C NMR (62.5 MHz, DMSO-*d*₆) δ (ppm): 49.4, 108.8, 111.2, 118.1, 119.0, 119.5, 121.1, 122.5, 124.8, 127.1, 127.6, 128.6, 129.3, 136.5, 137.4, 145.7, 146.8, 156.8, 158.6. HRMS (APCI): *m/z* calcd for C₂₁H₁₆N₃OS: 358.1009; found: 358.1005.

4.1.16. 4-Chloro-6-(1H-indol-3-yl)thieno[3,2-*d*]pyrimidine (**45a**)

To a solution of dry DMF (5 mL) was added dropwise phosphorus oxychloride (0.47 mL, 5 mmol) at 0 °C. After few minutes of stirring, 6-(1H-indol-3-yl)thieno[3,2-*d*]pyrimidin-4(3H)-one **44a** (267 mg, 1 mmol) dissolved in DMF (5 mL) was added dropwise at 0 °C. The reaction mixture was heated at 50 °C overnight. After cooling, the solution was poured into ice-water (100 mL) and the precipitate was filtered and washed several times with cold water. The crude product was purified by silica gel column chromatography (cyclohexane:AcOEt = 60:40) to provide a yellow solid (129 mg, 0.45 mmol, 45%); mp 274 °C. ¹H NMR (250 MHz, DMSO-*d*₆) δ (ppm): 7.47–7.54 (m, 2H, 2× CH), 8.11–8.18 (m, 2H, 2× CH), 8.29–8.35 (m, 1H, CH), 8.61 (s, 1H, CH), 9.01 (s, 1H, CH), 9.52 (s, 1H, NH). ¹³C NMR (62.5 MHz, DMSO-*d*₆) δ (ppm): 120.1, 120.8, 121.2, 121.6, 122.3, 125.0, 125.6, 127.2, 136.7, 142.4, 147.1, 156.5, 156.8, 157.8. HRMS (ESI): *m/z* calcd for C₁₄H₉ClN₃S: 286.0200; found: 286.0194.

4.1.17. 6-(1-Benzyl-1H-indol-3-yl)-4-chlorothieno[3,2-*d*]pyrimidine (**45b**)

This compound was synthesized using the same procedure as for **45a** starting with 6-(1-benzyl-1H-indol-3-yl)thieno[3,2-*d*]pyrimidin-4(3H)-one **44b**. The crude product was triturated in petroleum ether and filtered to afford yellow solid (368 mg, 0.98 mmol, 98%); mp 163 °C. ¹H NMR (250 MHz, DMSO-*d*₆) δ (ppm): 5.62 (s, 2H, CH₂), 7.27–7.39 (m, 7H, 7× CH), 7.67–7.73 (m, 1H, CH), 8.06–8.12 (m, 1H, CH), 8.96 (s, 1H, CH), 9.10 (s, 1H, CH), 10.41 (s, 1H, CH). ¹³C NMR (62.5 MHz, DMSO-*d*₆) δ (ppm): 49.6, 106.8, 111.6, 119.3, 121.8, 123.1, 125.57, 125.64, 127.3, 127.7, 128.7, 134.1, 136.4, 137.0, 148.0, 153.6, 156.5, 157.5, 162.2. HRMS (ESI): *m/z* calcd for C₂₁H₁₅ClN₃S: 376.0670; found: 376.0679.

4.1.18. 6-(1-Benzyl-1H-indol-3-yl)-4-(4-methoxyphenoxy)thieno[3,2-*d*]pyrimidine (**1a**)

Preparation of 4-methoxyphenolate. In round bottom flask was placed sodium hydroxide (200 mg, 5 mmol) in water (1 mL). Then, *p*-methoxyphenol (621 mg, 5 mmol) was added to the solution. After

dissolution, the reaction mixture was dried under reduce pressure to give quantitative white solid. *Preparation of the title compound.* To a solution of 6-(1-benzyl-1H-indol-3-yl)-4-chlorothieno[3,2-*d*]pyrimidine **45b** (376 mg, 1 mmol) in dry DMF (5 mL) was added 4-methoxyphenolate (292 mg, 2 mmol) freshly prepared. The reaction mixture was stirred at room temperature overnight. The solution was poured into ice-water (100 mL) and the precipitate was filtered and washed with water. The crude product was purified by silica gel column chromatography (cyclohexane:AcOEt = 80:20) to provide yellow solid (375 mg, 0.81 mmol, 81%); mp 174 °C. ¹H NMR (250 MHz, DMSO-*d*₆) δ (ppm): 3.79 (s, 3H, CH₃), 5.52 (s, 2H, CH₂), 7.01 (d, 2H, 2× CH, *J* = 9.1 Hz), 7.23–7.35 (m, 9H, 9× CH), 7.59–7.62 (m, 1H, CH), 7.83 (s, 1H, CH), 8.06–8.10 (m, 1H, CH), 8.41 (s, 1H, CH), 8.62 (s, 1H, CH). ¹³C NMR (62.5 MHz, DMSO-*d*₆) δ (ppm): 49.5, 55.4, 108.5, 111.4, 113.8, 114.6, 116.4, 119.6, 121.4, 122.7, 122.9, 124.9, 127.2, 127.6, 128.6, 130.2, 136.6, 137.3, 145.2, 147.5, 154.4, 157.0, 163.0, 164.0. HRMS (APCI): *m/z* calcd for C₂₈H₂₂N₃O₂S: 464.1427; found: 464.1432.

4.1.19. 6-(1-Benzyl-1H-indol-3-yl)-4-(4-methyl-1-piperazinyl)thieno[3,2-*d*]pyrimidine (**1b**)

A solution of 6-(1-benzyl-1H-indol-3-yl)-4-chlorothieno[3,2-*d*]pyrimidine **45b** (38 mg, 0.1 mmol) in few drops of *N*-methylpiperazine was stirred at room temperature overnight. Then, water (10 mL) was added to the solution. The aqueous layer was extracted twice with AcOEt (10 mL). The organic layer was washed once with hydrochloric acid 1 N (10 mL) and once with brine (10 mL), dried over MgSO₄ and concentrated under reduce pressure to provide yellow solid (15 mg, 0.034 mmol, 34%); mp 110 °C. ¹H NMR (250 MHz, acetone-*d*₆) δ (ppm): 2.29 (s, 3H, CH₃), 2.52–2.56 (m, 4H, 2× CH₂), 4.02–4.11 (m, 4H, 2× CH₂), 5.69 (s, 2H, CH₂), 7.24–7.38 (m, 7H, 7× CH), 7.58–7.63 (m, 1H, CH), 8.15–8.21 (m, 1H, CH), 8.56 (s, 1H, CH), 8.94 (s, 1H, CH), 10.62 (s, 1H, CH). ¹³C NMR (62.5 MHz, acetone-*d*₆) δ (ppm): 46.2, 46.8, 51.1, 55.6, 108.0, 112.0, 112.2, 121.4, 122.6, 123.9, 125.2, 127.4, 128.2, 128.7, 129.6, 135.9, 137.8, 138.0, 152.4, 155.5, 158.1, 186.4. HRMS (ESI): *m/z* calcd for C₂₆H₂₆N₅S: 440.1903; found: 440.1911.

4.1.20. 6-(1-Benzyl-1H-indol-3-yl)-4-chlorothieno[3,2-*d*][1,2,3]triazine (**46**)

To a solution of 3-amino-5-(1-benzyl-1H-indol-3-yl)-2-thiophenecarbonitrile **43e** (659 mg, 2 mmol) in concentrated hydrochloric acid (6 mL) was added dropwise sodium nitrite (193 mg, 2.80 mmol) dissolved in water (5 mL). After addition, the reaction mixture was stirred at room temperature overnight. The solution was poured into ice-water (150 mL) and the precipitate was filtered and washed with water. The residue was purified by silica gel column chromatography (cyclohexane:AcOEt = 90:10) to afford yellow solid (663 mg, 1.76 mmol, 88%); mp 173 °C. ¹H NMR (250 MHz, CDCl₃) δ (ppm): 5.43 (s, 2H, CH₂), 7.20–7.24 (m, 2H, 2× CH), 7.33–7.45 (m, 6H, 6× CH), 7.71 (s, 1H, CH), 7.93 (s, 1H, CH), 8.07–8.11 (m, 1H, CH). ¹³C NMR (62.5 MHz, CDCl₃) δ (ppm): 50.8, 109.2, 111.0, 115.1, 119.9, 122.5, 123.9, 125.4, 127.1, 127.4, 128.4, 129.0, 129.2, 129.5, 135.6, 137.4, 138.3, 150.9. HRMS (APCI): *m/z* calcd for C₂₀H₁₄ClN₄S: 377.0622; found: 377.0634.

4.1.21. 6-(1-Benzyl-1H-indol-3-yl)-4-(4-methoxybenzyl)thieno[3,2-*d*][1,2,3]triazine (**1c**)

[This compound was synthesized using the same procedure as for **1a** starting with 6-(1-benzyl-1H-indol-3-yl)-4-chlorothieno[3,2-*d*][1,2,3]triazine **46** and 4-methoxyphenolate. The residue was purified by silica gel column chromatography (cyclohexane:AcOEt = 80:20) to afford yellow solid (372 mg, 0.80 mmol, 80%); mp 165 °C. ¹H NMR (250 MHz, DMSO-*d*₆) δ (ppm): 3.81 (s, 3H, CH₃), 5.54 (s, 2H, CH₂), 7.07 (d, 2H, 2× CH, *J* = 9.0 Hz), 7.26–7.38 (m, 9H, 9× CH), 7.61–7.64 (m, 1H,

CH), 8.08–8.12 (m, 1H, CH), 8.17 (s, 1H, CH), 8.52 (s, 1H, CH). ^{13}C NMR (62.5 MHz, DMSO- d_6) δ (ppm): 49.6, 55.5, 107.8, 111.5, 114.4, 114.6, 114.8, 119.6, 121.7, 122.9, 123.0, 124.7, 127.2, 127.7, 128.7, 131.2, 136.7, 137.1, 144.9, 149.3, 157.4, 159.8, 160.1. HRMS (APCI): m/z calcd for $\text{C}_{27}\text{H}_{21}\text{N}_4\text{O}_2\text{S}$: 465.1380; found: 465.1372.

4.1.22. 3-[(Chloroacetyl)amino]-5-(1H-indol-3-yl)-2-thiophenecarboxamide (**47a**)

To a solution of 3-amino-5-(1H-indol-3-yl)-2-thiophenecarboxamide **43c** (772 mg, 3 mmol) and Et_3N (500 μL , 3.6 mmol) in dry THF was added dropwise chloroacetyl chloride (286 μL , 3.6 mmol) diluted in THF (2 mL) at 0 °C. The ice-bath was removed and the reaction mixture was stirred at room temperature 2 h. Then, the solution was poured into ice-water (30 mL) and the precipitate was filtered and washed once with cold water and once with petroleum ether to afford a yellow solid (411 mg, 1.23 mmol, 41%); mp 246 °C; IR (neat): 1652 (C=O), 2369, 2931, 3278 (NH + NH $_2$) cm^{-1} . ^1H NMR (250 MHz, DMSO- d_6) δ (ppm): 4.47 (s, 2H, CH $_2$), 7.16–7.24 (m, 2H, 2 \times CH), 7.41–7.46 (m, 1H, CH), 7.60 (br s, 2H, NH $_2$), 7.86–7.93 (m, 1H, CH), 7.93 (s, 1H, CH), 8.19 (s, 1H, CH), 11.69 (br s, 1H, NH), 12.04 (br s, 1H, NH). ^{13}C NMR (62.5 MHz, DMSO- d_6) δ (ppm): 43.1, 108.8, 109.4, 112.4, 115.0, 118.7, 120.4, 122.2, 124.2, 125.1, 136.6, 140.8, 142.1, 164.0, 164.4. HRMS (ESI): m/z calcd for $\text{C}_{15}\text{H}_{12}\text{ClN}_3\text{O}_2\text{SNa}$: 356.0231; found: 356.0236.

4.1.23. 5-(1-Benzyl-1H-indol-3-yl)-3-[(chloroacetyl)amino]-2-thiophenecarboxamide (**47b**)

This compound was synthesized using the same procedure as for **47a** starting with 3-amino-5-(1-benzyl-1H-indol-3-yl)-2-thiophenecarboxamide **43f** to afford a yellow solid (1.07 g, 2.52 mmol, 84%); mp 183 °C; IR (neat): 1652 (C=O), 2360, 3094 (NH + NH $_2$) cm^{-1} . ^1H NMR (250 MHz, DMSO- d_6) δ (ppm): 4.47 (s, 2H, CH $_2$), 5.49 (s, 2H, CH $_2$), 7.20–7.31 (m, 7H, 7 \times CH), 7.56–7.59 (m, 1H, CH), 7.60 (br s, 2H, NH $_2$), 7.87–7.91 (m, 1H, CH), 8.19 (s, 1H, CH), 8.21 (s, 1H, CH), 12.04 (br s, 1H, NH). ^{13}C NMR (62.5 MHz, DMSO- d_6) δ (ppm): 43.1, 49.3, 108.5, 109.6, 111.3, 115.1, 119.0, 120.8, 122.5, 124.8, 127.2, 127.5, 128.4, 128.6, 136.4, 137.5, 140.1, 142.1, 164.0, 165.4. HRMS (ESI): m/z calcd for $\text{C}_{22}\text{H}_{18}\text{ClN}_3\text{O}_2\text{SNa}$: 446.0700; found: 446.0713.

4.1.24. 5-(1H-Indol-3-yl)-3-[(1-piperidinylacetyl)amino]-2-thiophenecarboxamide (**48a**)

A solution of 3-[(chloroacetyl)amino]-5-(1H-indol-3-yl)-2-thiophenecarboxamide **47a** (80 mg, 0.24 mmol), piperidine (24 μL , 0.24 mmol) and dry potassium carbonate (33 mg, 0.24 mmol) in dry CH_3CN (3 mL) was heated at reflux 1 h. After cooling, the reaction mixture was poured into ice-water (30 mL) and the precipitate was filtered and washed once with cold water and once with petroleum ether to give a pale red solid (91 mg, 0.238 mmol, 99%); mp 247 °C; IR (neat): 1667 (C=O), 2359, 2930, 3166 (NH + NH $_2$) cm^{-1} . ^1H NMR (250 MHz, DMSO- d_6) δ (ppm): 1.35–1.45 (m, 2H, CH $_2$), 1.58–1.68 (m, 4H, 2 \times CH $_2$), 2.42–2.48 (m, 4H, 2 \times CH $_2$), 3.08 (s, 2H, CH $_2$), 7.17–7.21 (m, 2H, 2 \times CH), 7.46–7.49 (m, 3H, NH $_2$ + CH), 7.87–7.89 (m, 2H, 2 \times CH), 8.29 (s, 1H, CH), 11.66 (br s, 1H, NH), 12.17 (br s, 1H, NH). ^{13}C NMR (62.5 MHz, DMSO- d_6) δ (ppm): 23.4, 25.3, 54.3, 62.3, 108.7, 109.0, 112.4, 115.3, 118.7, 120.3, 122.1, 124.3, 124.7, 136.6, 140.1, 142.5, 165.2, 168.6. HRMS (ESI): m/z calcd for $\text{C}_{20}\text{H}_{23}\text{N}_4\text{O}_2\text{S}$: 383.1536; found: 383.1529.

4.1.25. 5-(1H-Indol-3-yl)-3-[(4-morpholinylacetyl)amino]-2-thiophenecarboxamide (**48b**)

This compound was synthesized using the same procedure as for **48a** starting with 3-[(chloroacetyl)amino]-5-(1H-indol-3-yl)-2-thiophenecarboxamide **47a** and morpholine to afford a beige solid (91 mg, 0.238 mmol, 99%); mp 261 °C; IR (neat): 1643 (C=O), 2808,

3150, 3277 (NH + NH $_2$) cm^{-1} . ^1H NMR (250 MHz, DMSO- d_6) δ (ppm): 2.49–2.51 (m, 4H, 2 \times CH $_2$), 3.15 (s, 2H, CH $_2$), 3.69–3.73 (m, 4H, 2 \times CH $_2$), 7.17–7.21 (m, 2H, 2 \times CH), 7.46–7.49 (m, 3H, NH $_2$ + CH), 7.85–7.88 (m, 2H, 2 \times CH), 8.28 (s, 1H, CH), 11.66 (br s, 1H, NH), 12.21 (br s, 1H, NH). ^{13}C NMR (62.5 MHz, DMSO- d_6) δ (ppm): 53.3, 61.6, 66.1, 108.8, 109.0, 112.4, 115.3, 118.7, 120.3, 122.1, 124.2, 124.8, 136.6, 140.2, 142.4, 165.3, 168.0. HRMS (ESI): m/z calcd for $\text{C}_{19}\text{H}_{21}\text{N}_4\text{O}_3\text{S}$: 385.1329; found: 385.1337.

4.1.26. 5-(1H-Indol-3-yl)-3-[(4-methyl-1-piperazinyl)acetyl]amino]-2-thiophenecarboxamide (**48c**)

This compound was synthesized using the same procedure as for **48a** starting with 3-[(chloroacetyl)amino]-5-(1H-indol-3-yl)-2-thiophenecarboxamide **47a** and *N*-methylpiperazine to afford a pale red solid (93 mg, 0.235 mmol, 98%); mp 258 °C; IR (neat): 1658 (C=O), 2808, 3159, 3258 (NH + NH $_2$) cm^{-1} . ^1H NMR (250 MHz, DMSO- d_6) δ (ppm): 2.18 (s, 3H, CH $_3$), 2.44–2.47 (m, 8H, 4 \times CH $_2$), 3.12 (s, 2H, CH $_2$), 7.14–7.20 (m, 2H, 2 \times CH), 7.43–7.50 (m, 3H, NH $_2$ + CH), 7.83–7.88 (m, 2H, 2 \times CH), 8.27 (s, 1H, CH), 11.64 (br s, 1H, NH), 12.05 (br s, 1H, NH). ^{13}C NMR (62.5 MHz, DMSO- d_6) δ (ppm): 45.6, 52.8, 54.3, 61.4, 108.8, 108.9, 112.4, 115.4, 118.7, 120.3, 122.1, 124.2, 124.7, 136.6, 140.1, 142.4, 165.2, 168.1. HRMS (ESI): m/z calcd for $\text{C}_{20}\text{H}_{24}\text{N}_5\text{O}_2\text{S}$: 398.1645; found: 398.1645.

4.1.27. 3-[(4-Benzyl-1-piperazinyl)acetyl]amino]-5-(1H-indol-3-yl)-2-thiophenecarboxamide (**48d**)

This compound was synthesized using the same procedure as for **48a** starting with 3-[(chloroacetyl)amino]-5-(1H-indol-3-yl)-2-thiophenecarboxamide **47a** and *N*-benzylpiperazine to provide a pale brown solid (113 mg, 0.238 mmol, 99%); mp 268 °C; IR (neat): 1644 (C=O), 2360, 2812, 3275 (NH + NH $_2$) cm^{-1} . ^1H NMR (250 MHz, DMSO- d_6) δ (ppm): 2.49–2.51 (m, 8H, 4 \times CH $_2$), 3.15 (s, 2H, CH $_2$), 3.47 (s, 2H, CH $_2$), 7.17–7.32 (m, 7H, 7 \times CH), 7.46–7.49 (m, 3H, NH $_2$ + CH), 7.86–7.89 (m, 2H, 2 \times CH), 8.29 (s, 1H, CH), 11.65 (br s, 1H, NH), 12.08 (br s, 1H, NH). ^{13}C NMR (62.5 MHz, DMSO- d_6) δ (ppm): 52.5, 53.0, 61.5, 62.0, 108.8, 109.0, 112.4, 115.4, 118.7, 120.3, 122.1, 124.2, 124.7, 126.9, 128.1, 128.7, 136.6, 138.5, 140.1, 142.4, 165.2, 168.1. HRMS (ESI): m/z calcd for $\text{C}_{26}\text{H}_{28}\text{N}_5\text{O}_2\text{S}$: 474.1958; found: 474.1981.

4.1.28. 5-(1H-Indol-3-yl)-3-[(1-pyrrolidinylacetyl)amino]-2-thiophenecarboxamide (**48e**)

This compound was synthesized using the same procedure as for **48a** starting with 3-[(chloroacetyl)amino]-5-(1H-indol-3-yl)-2-thiophenecarboxamide **47a** and pyrrolidine to provide a yellow solid (87 mg, 0.235 mmol, 98%); mp 237 °C; IR (neat): 1672 (C=O), 2853, 2957, 3219 (NH + NH $_2$) cm^{-1} . ^1H NMR (250 MHz, DMSO- d_6) δ (ppm): 1.74–1.83 (m, 4H, 2 \times CH $_2$), 2.61–2.69 (m, 4H, 2 \times CH $_2$), 3.32 (s, 2H, CH $_2$), 7.16–7.23 (m, 2H, 2 \times CH), 7.45–7.50 (m, 3H, NH $_2$ + CH), 7.85–7.90 (m, 2H, 2 \times CH), 8.26 (s, 1H, CH), 11.66 (br s, 1H, NH), 12.03 (br s, 1H, NH). ^{13}C NMR (62.5 MHz, DMSO- d_6) δ (ppm): 23.5, 53.7, 58.7, 108.2, 108.8, 109.0, 112.4, 115.4, 118.7, 120.3, 122.2, 124.3, 124.8, 136.6, 140.2, 142.5, 165.3. HRMS (ESI): m/z calcd for $\text{C}_{19}\text{H}_{21}\text{N}_4\text{O}_2\text{S}$: 369.1380; found: 369.1380.

4.1.29. 5-(1-Benzyl-1H-indol-3-yl)-3-[(1-piperidinylacetyl)amino]-2-thiophenecarboxamide (**48f**)

This compound was synthesized using the same procedure as for **48a** starting with 5-(1-benzyl-1H-indol-3-yl)-3-[(chloroacetyl)amino]-2-thiophenecarboxamide **47b** and piperidine to afford a beige solid (104 mg, 0.221 mmol, 92%); mp 112 °C; IR (neat): 1644 (C=O), 2933, 3176 (NH + NH $_2$) cm^{-1} . ^1H NMR (250 MHz, CDCl_3) δ (ppm): 1.35–1.47 (m, 2H, CH $_2$), 1.61–1.72 (m, 4H, 2 \times CH $_2$), 2.43–2.52 (m, 4H, 2 \times CH $_2$), 3.08 (s, 2H, CH $_2$), 5.28 (s, 2H, CH $_2$), 5.39 (sl, 2H, NH $_2$), 7.07–7.29 (m, 8H, 8 \times CH), 7.47 (s, 1H, CH), 7.94–8.02 (m, 1H, CH), 8.36 (s, 1H, CH), 11.93 (br s, 1H, NH). ^{13}C NMR (62.5 MHz, CDCl_3) δ (ppm): 23.9,

26.0, 50.4, 55.1, 63.0, 107.9, 110.2, 110.3, 117.3, 120.2, 121.1, 122.9, 125.7, 127.0, 127.3, 128.0, 129.0, 136.4, 137.0, 140.6, 143.9, 165.5, 169.8. HRMS (ESI): m/z calcd for $C_{27}H_{29}N_4O_2S$: 473.2006; found: 473.2006.

4.1.30. 5-(1-Benzyl-1H-indol-3-yl)-3-[(4-morpholinylacetyl)amino]-2-thiophenecarboxamide (48g)

This compound was synthesized using the same procedure as for **48a** starting with 5-(1-benzyl-1H-indol-3-yl)-3-[(chloroacetyl)amino]-2-thiophenecarboxamide **47b** and morpholine to afford a beige solid (105 mg, 0.221 mmol, 92%); mp 116 °C; IR (neat): 1645 (C=O), 2816, 3188 (NH + NH₂) cm⁻¹. ¹H NMR (250 MHz, CDCl₃) δ (ppm): 2.62–2.65 (m, 4H, 2× CH₂), 3.21 (s, 2H, CH₂), 3.85–3.89 (m, 4H, 2× CH₂), 5.33 (s, 2H, CH₂), 5.57 (sl, 2H, NH₂), 7.15–7.35 (m, 8H, 8× CH), 7.52 (s, 1H, CH), 8.01–8.06 (m, 1H, CH), 8.41 (s, 1H, CH), 12.04 (br s, 1H, NH). ¹³C NMR (62.5 MHz, CDCl₃) δ (ppm): 50.4, 53.8, 62.5, 67.0, 108.0, 110.1, 110.4, 117.1, 120.2, 121.1, 123.0, 125.6, 127.0, 127.3, 128.0, 129.0, 136.4, 137.0, 140.9, 143.7, 165.6, 168.7. HRMS (ESI): m/z calcd for $C_{26}H_{26}N_4O_3SNa$: 497.1618; found: 497.1610.

4.1.31. 5-(1-Benzyl-1H-indol-3-yl)-3-[(4-methyl-1-piperazinyl)acetyl]amino-2-thiophene-carboxamide (48h)

This compound was synthesized using the same procedure as for **48a** starting with 5-(1-benzyl-1H-indol-3-yl)-3-[(chloroacetyl)amino]-2-thiophenecarboxamide **47b** and *N*-methylpiperazine to afford a beige solid (99 mg, 0.204 mmol, 85%); mp 128 °C; IR (neat): 1644 (C=O), 2799, 3192 (NH + NH₂) cm⁻¹. ¹H NMR (250 MHz, DMSO-*d*₆) δ (ppm): 2.36 (s, 3H, CH₃), 2.59–2.72 (m, 8H, 4× CH₂), 3.22 (s, 2H, CH₂), 5.34 (s, 2H, CH₂), 5.47 (sl, 2H, NH₂), 7.15–7.36 (m, 8H, 8× CH), 7.53 (s, 1H, CH), 8.02–8.06 (m, 1H, CH), 8.41 (s, 1H, CH), 11.92 (br s, 1H, NH). ¹³C NMR (62.5 MHz, DMSO-*d*₆) δ (ppm): 45.9, 50.4, 53.4, 54.9, 62.1, 108.0, 110.1, 110.3, 117.3, 120.2, 121.1, 122.9, 125.6, 127.0, 127.3, 128.0, 129.0, 136.4, 137.0, 140.7, 143.8, 165.4, 169.0. HRMS (ESI): m/z calcd for $C_{27}H_{30}N_5O_2S$: 488.2115; found: 488.2119.

4.1.32. 5-(1-Benzyl-1H-indol-3-yl)-3-[(4-benzyl-1-piperazinyl)acetyl]amino-2-thiophenecarboxamide (48i)

This compound was synthesized using the same procedure as for **48a** starting with 5-(1-benzyl-1H-indol-3-yl)-3-[(chloroacetyl)amino]-2-thiophenecarboxamide **47b** and *N*-benzylpiperazine to afford a beige solid (134 mg, 0.238 mmol, 99%); mp 204 °C; IR (neat): 1658 (C=O), 2816, 3182 (NH₂) cm⁻¹. ¹H NMR (250 MHz, DMSO-*d*₆) δ (ppm): 2.60–2.71 (m, 8H, 4× CH₂), 3.21 (s, 2H, CH₂), 3.59 (s, 2H, CH₂), 5.34 (s, 2H, CH₂), 5.51 (sl, 2H, NH₂), 7.15–7.37 (m, 13H, 13× CH), 7.53 (s, 1H, CH), 8.02–8.06 (m, 1H, CH), 8.41 (s, 1H, CH), 11.94 (br s, 1H, NH). ¹³C NMR (62.5 MHz, DMSO-*d*₆) δ (ppm): 50.4, 53.1, 53.5, 62.2, 62.8, 108.0, 110.1, 110.3, 117.3, 120.2, 121.1, 122.9, 125.6, 126.98, 126.99, 127.1, 127.3, 128.0, 128.2, 129.0, 129.2, 136.4, 137.0, 140.7, 143.8, 165.5, 169.1. HRMS (ESI): m/z calcd for $C_{33}H_{34}N_5O_2S$: 564.2428; found: 564.2453.

4.1.33. 5-(1-Benzyl-1H-indol-3-yl)-3-[(1-pyrrolidinylacetyl)amino]-2-thiophenecarboxamide (48j)

This compound was synthesized using the same procedure as for **48a** starting with 5-(1-benzyl-1H-indol-3-yl)-3-[(chloroacetyl)amino]-2-thiophenecarboxamide **47b** and pyrrolidine to afford a beige solid (108 mg, 0.235 mmol, 98%); mp 180 °C; IR (neat): 1662 (C=O), 2787, 3149 (NH + NH₂) cm⁻¹. ¹H NMR (250 MHz, DMSO-*d*₆) δ (ppm): 1.81–1.89 (m, 4H, 2× CH₂), 2.63–2.70 (s, 4H, 2× CH₂), 3.35 (s, 2H, CH₂), 5.28 (s, 2H, CH₂), 5.39 (sl, 2H, NH₂), 7.08–7.30 (m, 8H, 8× CH), 7.46 (s, 1H, CH), 7.95–8.00 (m, 1H, CH), 8.35 (s, 1H, CH), 11.86 (br s, 1H, NH). ¹³C NMR (62.5 MHz, DMSO-*d*₆) δ (ppm): 24.2, 50.4, 54.5, 59.6, 107.8, 110.1, 110.3, 117.3, 120.2, 121.1, 122.9, 125.6, 127.0, 127.3, 128.0, 129.0, 136.4, 137.0, 140.7, 144.0, 165.6, 169.7. HRMS (ESI): m/z calcd for $C_{26}H_{27}N_4O_2S$: 459.1849; found: 459.1867.

4.1.34. 6-(1H-Indol-3-yl)-2-(1-piperidinylmethyl)thieno[3,2-*d*]pyrimidin-4(3H)-one (2a)

To a solution of 5-(1H-Indol-3-yl)-3-[(1-piperidinylacetyl)amino]-2-thiophenecarboxamide **48a** (36.0 mg, 0.1 mmol) in DMF (2.5 mL) was added NaOH 2 N (2.5 mL) and heated at reflux for 30 min. After cooling, the reaction mixture was poured into ice-water under good stirring. The precipitate was filtered, washed once with water and once with petroleum ether to provide a beige solid (35.7 mg, 0.098 mmol, 98%); mp 350 °C (dec.); IR (neat): 1660 (C=O), 2937 (NH) cm⁻¹. ¹H NMR (250 MHz, DMSO-*d*₆) δ (ppm): 1.31–1.33 (m, 2H, CH₂), 1.44–1.46 (m, 4H, 2× CH₂), 2.38–2.46 (m, 4H, 2× CH₂), 3.37 (s, 2H, CH₂), 7.12–7.17 (m, 2H, 2× CH), 7.44–7.47 (m, 1H, CH), 7.52 (s, 1H, CH), 7.90–7.93 (m, 1H, CH), 8.01 (s, 1H, CH), 8.44 (br s, 1H, NH), 12.03 (br s, 1H, NH). ¹³C NMR (62.5 MHz, DMSO-*d*₆) δ (ppm): 23.6, 25.4, 53.8, 61.0, 109.0, 112.4, 117.2, 117.6, 119.0, 120.7, 122.2, 124.1, 125.9, 136.8, 146.5, 156.3, 157.6, 158.4. HRMS (ESI): m/z calcd for $C_{20}H_{21}N_4OS$: 365.1431; found: 365.1431.

4.1.35. 6-(1H-Indol-3-yl)-2-(4-morpholinylmethyl)thieno[3,2-*d*]pyrimidin-4(3H)-one (2b)

This compound was synthesized using the same procedure as for **2a** starting with 5-(1H-Indol-3-yl)-3-[(4-morpholinylacetyl)amino]-2-thiophenecarboxamide **48b** to afford a beige solid (35.9 mg, 0.098 mmol, 98%); mp 262 °C; IR (neat): 1652 (C=O), 2835 (NH) cm⁻¹. ¹H NMR (250 MHz, DMSO-*d*₆) δ (ppm): 2.47–2.51 (m, 2H, CH₂), 3.31–3.36 (m, 2H, CH₂), 3.46 (s, 2H, CH₂), 3.57–3.61 (m, 4H, 2× CH₂), 7.18–7.22 (m, 2H, 2× CH), 7.48–7.51 (m, 1H, CH), 7.57 (s, 1H, CH), 7.95–7.98 (m, 1H, CH), 8.06 (s, 1H, CH), 8.49 (br s, 1H, NH), 11.90 (br s, 1H, NH). ¹³C NMR (62.5 MHz, DMSO-*d*₆) δ (ppm): 53.0, 60.5, 66.1, 109.0, 112.4, 117.4, 117.6, 119.0, 120.7, 122.2, 124.1, 126.0, 136.7, 146.5, 155.7, 157.5, 158.3. HRMS (ESI): m/z calcd for $C_{19}H_{18}N_4O_2SNa$: 389.1043; found: 389.1045.

4.1.36. 6-(1H-Indol-3-yl)-2-[(4-methyl-1-piperazinyl)methyl]thieno[3,2-*d*]pyrimidin-4(3H)-one (2c)

This compound was synthesized using the same procedure as for **2a** starting with 5-(1H-Indol-3-yl)-3-[(4-methyl-1-piperazinyl)acetyl]amino-2-thiophenecarboxamide **48c** to afford a beige solid (36.8 mg, 0.097 mmol, 97%); mp 350 °C (dec.); IR (neat): 1651 (C=O), 3125 (NH) cm⁻¹. ¹H NMR (250 MHz, DMSO-*d*₆) δ (ppm): 2.45 (m, 3H, CH₃), 2.66–2.71 (m, 4H, 2× CH₂), 2.75–2.81 (m, 4H, 2× CH₂), 3.52 (s, 2H, CH₂), 7.15–7.24 (m, 2H, 2× CH), 7.48–7.52 (m, 1H, CH), 7.57 (s, 1H, CH), 7.94–7.97 (m, 1H, NH), 8.06 (s, 1H, NH), 8.18 (s, 1H, CH), 12.04 (br s, 1H, NH). ¹³C NMR (62.5 MHz, DMSO-*d*₆) δ (ppm): 43.1, 50.1, 52.9, 59.4, 109.0, 112.5, 117.4, 117.6, 118.8, 120.7, 122.3, 124.1, 126.0, 136.7, 146.6, 155.6, 157.4, 158.2. HRMS (ESI): m/z calcd for $C_{20}H_{22}N_5OS$: 380.1540; found: 380.1549.

4.1.37. 2-[(4-Benzyl-1-piperazinyl)methyl]-6-(1H-indol-3-yl)thieno[3,2-*d*]pyrimidin-4(3H)-one (2d)

This compound was synthesized using the same procedure as for **2a** starting with 3-[(4-benzyl-1-piperazinyl)acetyl]amino-5-(1H-indol-3-yl)-2-thiophenecarboxamide **48d** to afford a beige solid (44.2 mg, 0.097 mmol, 97%); mp 350 °C (dec.); IR (neat): 1659 (C=O), 2815 (NH) cm⁻¹. ¹H NMR (250 MHz, DMSO-*d*₆) δ (ppm): 2.34–2.42 (m, 4H, 2× CH₂), 2.46–2.53 (m, 4H, 2× CH₂), 3.44 (s, 2H, CH₂), 3.46 (s, 2H, CH₂), 7.14–7.33 (m, 7H, 7× CH), 7.47–7.52 (m, 1H, CH), 7.56 (s, 1H, CH), 7.92–7.98 (m, 1H, CH), 8.04 (s, 1H, CH), 8.47 (br s, 1H, NH), 12.12 (br s, 1H, NH). ¹³C NMR (62.5 MHz, DMSO-*d*₆) δ (ppm): 52.4, 52.6, 60.2, 62.0, 109.0, 112.4, 117.3, 117.6, 119.0, 120.7, 122.2, 124.1, 125.9, 126.8, 128.1, 128.8, 136.8, 138.1, 146.4, 156.1, 157.7, 158.4. HRMS (ESI): m/z calcd for $C_{26}H_{26}N_5OS$: 456.1853; found: 456.1856.

4.1.38. 6-(1*H*-Indol-3-yl)-2-(1-pyrrolidinylmethyl)thieno[3,2-*d*]pyrimidin-4(3*H*)-one (**2e**)

This compound was synthesized using the same procedure as for **2a** starting with 5-(1*H*-indol-3-yl)-3-[(1-pyrrolidinylacetyl)amino]-2-thiophenecarboxamide **48e** to afford a beige solid (34.3 mg, 0.098 mmol, 98%); mp 350 °C (dec.); IR (neat): 1660 (C=O), 2817 (NH) cm⁻¹. ¹H NMR (250 MHz, DMSO-*d*₆) δ (ppm): 1.64–1.70 (m, 4H, 2 × CH₂), 2.47–2.55 (m, 4H, 2 × CH₂), 3.53 (s, 2H, CH₂), 7.09–7.21 (m, 2H, 2 × CH), 7.43–7.47 (m, 1H, CH), 7.52 (s, 1H, CH), 7.89–7.95 (m, 1H, CH), 8.01 (s, 1H, CH), 8.44 (br s, 1H, NH), 12.01 (br s, 1H, NH). ¹³C NMR (62.5 MHz, DMSO-*d*₆) δ (ppm): 23.5, 53.7, 57.9, 109.0, 112.4, 117.2, 117.6, 119.0, 120.7, 122.2, 124.2, 125.9, 136.7, 146.5, 156.7, 157.6, 158.5. HRMS (ESI): *m/z* calcd for C₁₉H₁₈N₄OSNa: 373.1094; found: 373.1101.

4.1.39. 6-(1-Benzyl-1*H*-indol-3-yl)-2-(1-piperidinylmethyl)thieno[3,2-*d*]pyrimidin-4(3*H*)-one (**2f**)

This compound was synthesized using the same procedure as for **2a** starting with 5-(1-benzyl-1*H*-indol-3-yl)-3-[(1-piperidinylacetyl)amino]-2-thiophenecarboxamide **48f** to afford a beige solid (45.0 mg, 0.099 mmol, 99%); mp 114 °C; IR (neat): 1667 (C=O), 2930 (NH) cm⁻¹. ¹H NMR (250 MHz, CDCl₃) δ (ppm): 1.38–1.48 (m, 2H, CH₂), 1.52–1.64 (m, 4H, 2 × CH₂), 2.44–2.52 (m, 4H, 2 × CH₂), 3.48 (s, 2H, CH₂), 5.32 (s, 2H, CH₂), 7.08–7.15 (m, 2H, 2 × CH), 7.18–7.30 (m, 6H, 6 × CH), 7.37 (s, 1H, CH), 7.48 (s, 1H, CH), 7.93–8.02 (m, 1H, CH), 10.02 (br s, 1H, NH). ¹³C NMR (62.5 MHz, CDCl₃) δ (ppm): 23.6, 25.8, 50.5, 54.8, 60.8, 110.4, 110.5, 118.4, 118.8, 120.0, 121.4, 123.1, 125.7, 126.9, 127.6, 128.0, 129.0, 136.3, 137.1, 147.3, 157.4, 159.0, 169.0. HRMS (ESI): *m/z* calcd for C₂₇H₂₇N₄OS: 455.1900; found: 455.1912.

4.1.40. 6-(1-Benzyl-1*H*-indol-3-yl)-2-(4-morpholinylmethyl)thieno[3,2-*d*]pyrimidin-4(3*H*)-one (**2g**)

This compound was synthesized using the same procedure as for **2a** starting with 5-(1-benzyl-1*H*-indol-3-yl)-3-[(4-morpholinylacetyl)amino]-2-thiophenecarboxamide **48g** to afford a beige solid (44.7 mg, 0.098 mmol, 98%); mp 236 °C; IR (neat): 1661 (C=O), 2848 (NH) cm⁻¹. ¹H NMR (250 MHz, CDCl₃) δ (ppm): 2.61–2.65 (m, 4H, 2 × CH₂), 3.61 (s, 2H, CH₂), 3.77–3.81 (m, 4H, 2 × CH₂), 5.35 (s, 2H, CH₂), 7.16–7.23 (m, 2H, 2 × CH), 7.28–7.37 (m, 6H, 6 × CH), 7.44 (s, 1H, CH), 7.56 (s, 1H, CH), 8.01–8.06 (m, 1H, CH), 10.07 (br s, 1H, NH). ¹³C NMR (62.5 MHz, CDCl₃) δ (ppm): 50.5, 53.6, 60.7, 66.8, 110.3, 110.5, 118.4, 118.7, 120.0, 121.5, 123.1, 125.6, 126.9, 127.6, 128.1, 129.0, 136.3, 137.1, 147.6, 155.0, 157.4, 158.9. HRMS (ESI): *m/z* calcd for C₂₆H₂₅N₄O₂S: 457.1693; found: 457.1676.

4.1.41. 6-(1-Benzyl-1*H*-indol-3-yl)-2-[(4-methyl-1-piperazinyl)methyl]thieno[3,2-*d*]pyrimidin-4(3*H*)-one (**2h**)

This compound was synthesized using the same procedure as for **2a** starting with 5-(1-benzyl-1*H*-indol-3-yl)-3-[(4-methyl-1-piperazinylacetyl)amino]-2-thiophenecarboxamide **48h** to afford a beige solid (46.5 mg, 0.099 mmol, 99%); mp 132 °C; IR (neat): 1660 (C=O), 2796 (NH) cm⁻¹. ¹H NMR (250 MHz, CDCl₃) δ (ppm): 2.33 (s, 3H, CH₃), 2.48–2.58 (m, 4H, 2 × CH₂), 2.63–2.71 (m, 4H, 2 × CH₂), 3.61 (s, 2H, CH₂), 5.38 (s, 2H, CH₂), 7.15–7.21 (m, 2H, 2 × CH), 7.24–7.38 (m, 6H, 6 × CH), 7.44 (s, 1H, CH), 7.55 (s, 1H, CH), 8.00–8.09 (m, 1H, CH), 10.01 (s, 1H, NH). ¹³C NMR (62.5 MHz, CDCl₃) δ (ppm): 45.9, 50.5, 53.5, 54.9, 60.2, 110.4, 110.5, 118.4, 118.7, 120.0, 121.4, 123.1, 125.7, 126.9, 127.6, 128.1, 129.0, 136.3, 137.1, 147.4, 155.4, 157.4, 159.0. HRMS (ESI): *m/z* calcd for C₂₇H₂₈N₅OS: 470.2009; found: 470.2008.

4.1.42. 6-(1-Benzyl-1*H*-indol-3-yl)-2-[(4-benzyl-1-piperazinyl)methyl]thieno[3,2-*d*]pyrimidin-4(3*H*)-one (**2i**)

This compound was synthesized using the same procedure as for **2a** starting with 5-(1-benzyl-1*H*-indol-3-yl)-3-[(4-benzyl-1-piperazinylacetyl)amino]-2-thiophenecarboxamide **48i** to afford

a beige solid (53.5 mg, 0.098 mmol, 98%); mp 350 °C (dec.); IR (neat): 1667 (C=O), 2814 (NH) cm⁻¹. ¹H NMR (250 MHz, CDCl₃) δ (ppm): 2.51–2.59 (m, 4H, 2 × CH₂), 2.62–2.69 (m, 4H, 2 × CH₂), 3.56 (s, 2H, CH₂), 3.61 (s, 2H, CH₂), 5.39 (s, 2H, CH₂), 7.15–7.22 (m, 2H, 2 × CH), 7.24–7.38 (m, 11H, 11 × CH), 7.43 (s, 1H, CH), 7.55 (s, 1H, CH), 8.03–8.07 (m, 1H, CH), 10.04 (s, 1H, NH). ¹³C NMR (62.5 MHz, CDCl₃) δ (ppm): 50.5, 52.9, 53.4, 60.2, 62.9, 110.4, 110.5, 118.4, 118.7, 120.0, 121.4, 123.1, 125.7, 126.9, 127.2, 127.6, 128.1, 128.3, 129.0, 129.2, 136.3, 137.1, 137.9, 147.4, 155.5, 157.4, 159.0. HRMS (ESI): *m/z* calcd for C₃₃H₃₂N₅OS: 546.2322; found: 546.2331.

4.1.43. 6-(1-Benzyl-1*H*-indol-3-yl)-2-(1-pyrrolidinylmethyl)thieno[3,2-*d*]pyrimidin-4(3*H*)-one (**2j**)

This compound was synthesized using the same procedure as for **2a** starting with 5-(1-benzyl-1*H*-indol-3-yl)-3-[(1-pyrrolidinylacetyl)amino]-2-thiophenecarboxamide **48j** to afford a beige solid (43.6 mg, 0.099 mmol, 99%); mp 212 °C; IR (neat): 1661 (C=O), 2809 (NH) cm⁻¹. ¹H NMR (250 MHz, CDCl₃) δ (ppm): 1.85–1.90 (m, 4H, 2 × CH₂), 2.66–2.73 (m, 4H, 2 × CH₂), 3.75 (s, 2H, CH₂), 5.38 (s, 2H, CH₂), 7.15–7.21 (m, 2H, 2 × CH), 7.26–7.36 (m, 6H, 6 × CH), 7.44 (s, 1H, CH), 7.55 (s, 1H, CH), 8.00–8.07 (m, 1H, CH), 8.43 (br s, 1H, NH). ¹³C NMR (62.5 MHz, CDCl₃) δ (ppm): 24.0, 50.5, 54.3, 57.4, 110.4, 110.5, 118.4, 118.6, 120.0, 121.4, 123.1, 125.7, 126.9, 127.6, 128.0, 129.0, 136.3, 137.1, 147.3, 156.3, 157.5, 159.1. HRMS (ESI): *m/z* calcd for C₂₆H₂₅N₄OS: 441.1744; found: 441.1734.

4.1.44. 6-(1-Benzyl-1*H*-indol-3-yl)-2-hexylthieno[3,2-*d*]pyrimidin-4-ol (**3a**)

To a solution of 3-amino-5-(1-benzyl-1*H*-indol-3-yl)-2-thiophenecarboxamide **43f** (347 mg, 1 mmol) in MeOH containing 6% of concentrated HCl, was added heptaldehyde (209 μL, 1.5 mmol). The reaction mixture was heated at reflux for 24 h. After cooling, the precipitate formed was filtered and washed once with cold MeOH to afford a yellow solid (93 mg, 0.21 mmol, 21%); mp 263 °C; IR (KBr): 2424 (OH) cm⁻¹. ¹H NMR (250 MHz, DMSO-*d*₆) δ (ppm): 0.83–0.87 (m, 3H, CH₃), 1.25–1.32 (m, 6H, 3 × CH₂), 1.71–1.74 (m, 2H, CH₂), 2.67–2.73 (t, 2H, CH₂, *J* = 7.43 Hz), 5.50 (s, 2H, CH₂), 7.21–7.29 (m, 7H, 7 × CH), 7.57–7.60 (m, 2H, 2 × CH), 7.95–7.98 (m, 1H, CH), 8.35 (s, 1H, CH). Proton of hydroxyl group exchange with deuterium of NMR solvent. ¹³C NMR (62.5 MHz, DMSO-*d*₆) δ (ppm): 13.9, 21.9, 27.0, 28.1, 30.8, 33.2, 48.5, 49.4, 108.6, 111.3, 116.0, 116.6, 119.4, 121.3, 122.6, 124.7, 127.2, 127.6, 128.6, 129.7, 136.5, 137.33, 146.7, 157.0, 160.5. HRMS (ESI): *m/z* calcd for C₂₇H₂₈N₃OS: 442.1948; found: 442.1963.

4.1.45. 6-(1-Benzyl-1*H*-indol-3-yl)-2-(4-methoxyphenyl)thieno[3,2-*d*]pyrimidin-4-ol (**3b**)

This compound was synthesized using the same procedure as for **3a** starting with 3-amino-5-(1-benzyl-1*H*-indol-3-yl)-2-thiophenecarboxamide **43f** and *p*-anisaldehyde to give a yellow solid (144 mg, 0.31 mmol, 31%); mp 278 °C; IR (KBr): 2518 (OH) cm⁻¹. ¹H NMR (250 MHz, DMSO-*d*₆) δ (ppm): 3.85 (s, 3H, CH₃), 5.51 (s, 2H, CH₂), 7.09 (d, 2H, 2 × CH, *J* = 8.93 Hz), 7.22–7.33 (m, 7H, 7 × CH), 7.56–7.60 (m, 1H, CH), 7.65 (s, 1H, CH), 8.00–8.04 (m, 1H, CH), 8.15 (d, 2 × CH, *J* = 8.93 Hz), 8.32 (s, 1H, CH). Proton of hydroxyl group exchange with deuterium of NMR solvent. ¹³C NMR (62.5 MHz, DMSO-*d*₆) δ (ppm): 49.4, 55.5, 108.8, 111.3, 114.0, 116.6, 117.7, 119.5, 121.2, 122.6, 124.1, 124.8, 127.2, 127.6, 128.6, 129.4, 129.6, 136.5, 137.4, 146.2, 154.3, 157.86, 157.93, 161.9. HRMS (ESI): *m/z* calcd for C₂₈H₂₂N₃O₂S: 464.1427; found: 464.1425.

4.1.46. 6-(1-Benzyl-1*H*-indol-3-yl)-2-(3,4,5-trimethoxyphenyl)thieno[3,2-*d*]pyrimidin-4-ol (**3c**)

This compound was synthesized using the same procedure as for **3a** starting with 3-amino-5-(1-benzyl-1*H*-indol-3-yl)-2-

thiophenecarboxamide **43f** and 3,4,5-trimethoxybenzaldehyde to provide a yellow solid (188 mg, 0.36 mmol, 36%); mp 289 °C; IR (KBr): 2939 (OH) cm^{-1} . ^1H NMR (250 MHz, DMSO- d_6) δ (ppm): 3.74 (s, 3H, CH₃), 3.89 (s, 6H, 2 \times CH₃), 5.51 (s, 2H, CH₂), 7.22–7.33 (m, 7H, 7 \times CH), 7.54 (s, 2H, 2 \times CH), 7.57–7.61 (m, 1H, CH), 7.69 (s, 1H, CH), 8.01–8.06 (m, 1H, CH), 8.32 (s, 1H, CH). Proton of hydroxyl group exchange with deuterium of NMR solvent. ^{13}C NMR (62.5 MHz, DMSO- d_6) δ (ppm): 49.4, 56.1, 60.1, 105.1, 108.9, 111.3, 117.0, 118.3, 119.6, 121.2, 122.7, 124.8, 127.2, 127.5, 127.6, 128.6, 136.5, 137.4, 140.1, 146.1, 152.8, 153.9, 158.0, 158.6. HRMS (ESI): m/z calcd for C₃₀H₂₆N₃O₄S: 524.1639; found: 524.1636.

4.1.47. 6-(1-Benzyl-1H-indol-3-yl)-2-(4-chlorophenyl)thieno[3,2-d]pyrimidin-4(3H)-one (**3d**)

This compound was synthesized using the same procedure as for **3a** starting with 3-amino-5-(1-benzyl-1H-indol-3-yl)-2-thiophenecarboxamide **43f** and *p*-chlorobenzaldehyde to afford a brown solid (56 mg, 0.12 mmol, 12%); mp 314 °C; IR (KBr): 1658 (C=O) cm^{-1} . ^1H NMR (250 MHz, DMSO- d_6) δ (ppm): 5.51 (s, 2H, CH₂), 7.22–7.33 (m, 7H, 7 \times CH), 7.55–7.67 (m, 5H, 5 \times CH), 8.00–8.06 (m, 1H, CH), 8.16 (d, 1H, CH, J = 8.65 Hz), 8.32 (s, 1H, CH), 12.72 (br s, 1H, NH). HRMS (APCI): m/z calcd for C₂₇H₁₉ClN₃O₃: 468.0932; found: 468.0939.

4.2. Molecular modeling, docking and 3-D QSAR predictions

All computational details will be detailed elsewhere [33]. Briefly all the molecules listed in Tables 1–3, 5 were modeled using the chemaxon msketch module (<http://www.chemaxon.com>) and directly used for the docking studies. AutoDock version 4.2 [45] was used and cross-docking experiments were carried out similarly as described by Musmuca [46]. The 3-D QSAR model was carried out using a in house procedure [47]. Nineteen VEGFR-2 co-crystallized complexes were retrieved from the PDB (www.rcsb.org), cleaned from any solvents and ions residues. The tyrosine phosphate non standard residue was kept in the structures. The complexes were subjected to a previous reported procedure for geometry optimization [46]. The minimized complex was aligned using Chimera 1.5.2 [48] and the ligands were then extracted obtaining the SB alignment. The AutoGrid module of the AutoDock suite was used to calculate the molecular interaction fields (MIFs) on the aligned molecules. The ligand MIFs and the corresponding activities were submitted to an R [49] script which performed PLS and cross-validations to assess the 3-D QSAR model.

SB alignment assessment was performed though extensive redocking and cross-docking experiments on the cleaned and minimized co-crystals. The modeled compounds **1–38** and the intermediates **44b**, **45b** and **48a–j** were then cross-docked. The built 3-D QSAR model was applied to lowest energy docked poses and the corresponding pIC₅₀ were predicted. The binding modes of the **1–38**, **44b**, **45b** and **48a–j** were analyzed by the mean of the Chimera software and the interaction profiles were obtained with the Ligplot software [50].

4.3. Biology. Materials and methods

Human recombinant protein tyrosine kinase VEGFR-2 and Omnia™ Tyr Peptide Kit 7 were from Invitrogen. Vandetanib, exploited as the reference standard, was from Sequoia research product Ltd.

4.3.1. Tyrosine kinase assays

Assays were performed in 96-well microtiter plates using the Omnia Tyr Peptide 7 Kit, according to the manufacturer's protocol and following a previously reported procedure, standardized for

EGFR [51]. Briefly, the kinase activity was determined fluorimetrically by monitoring the increase in fluorescence resulting from phosphorylation of the peptide substrate, carrying the fluorophore 8-hydroxy-5-(*N,N*-dimethylsulfonamido)-2-methylquinoline, catalyzed by VEGFR-2 in the presence of ATP.

Assays were carried out at 30 °C in a reaction mixture containing 5 μL of Tyrosine Kinase Reaction Buffer, 5 μL of Tyrosine Kinase Substrate, 5 μL of 1 mM ATP, 5 μL of 1 mM DTT, 25 μL of ultrapure water and 5 μL of 3 mU/ μL VEGFR-2, in a total volume of 50 μL . All the above reagents, except VEGFR-2, were incubated at 30 °C for 5 min. VEGFR-2 was then added to start the reaction, which was monitored with the fluorescence meter Victor3™ Perkin Elmer at 360 nm (excitation filter) and 485 nm (emission filter). Kinase activity was calculated from a linear least-squares fit of the data for fluorescence intensity versus time.

4.3.2. Enzymatic inhibition

The inhibitory activity of titled compounds against VEGFR-2 was assayed by adding 5 μL of the inhibitor solution to the reaction mixture described above. All the products were dissolved in 100% DMSO and diluted to the appropriate concentrations with Tyrosine Kinase Reaction Buffer, provided by the kit. Final concentration of DMSO in assay solutions never exceed 1%, and proved to have no effects on protein activity. The inhibitory effect of the new derivatives was routinely estimated at a concentration of 200 μM . Results are expressed as means \pm SEM of percentage inhibition values, obtained through two determinations carried out in triplicate (Tables 1–3, 5). Those compounds found to be active were then tested at additional concentrations between 200 μM and 20 nM. For a proper comparison Vandetanib was employed as the reference standard. The determination of the IC₅₀ values was performed by linear regression analysis of the log–dose response curve, which was generated using at least five concentrations of the inhibitor causing an inhibition between 20% and 80%, with three replicates at each concentration. Results are expressed as means \pm SEM (Table 4 compounds **2f** and **3d**). GraphPad 5.0 software was used for the statistical analysis.

4.3.3. Endothelial cell culture

Umbilical cords were cut after delivery in compliance with relevant laws in respect with consent of women. Rapidly, human umbilical vein endothelial cells (HUVEC) were collected from umbilical cords as previously described by Jaffe et al., 1973 [51]. HUVEC were cultured and used until passage 5 in "HUVEC/complete medium" consisting in 50% M199 (GibcoBRL, France) and 50% RPMI 1640 (v/v) (Sigma, France) supplemented with 20% heat inactivated human AB serum (EFS, Nancy, France), 2 mM L-glutamine (GibcoBRL), 100 U/mL penicillin (GibcoBRL, France), 100 $\mu\text{g}/\text{mL}$ streptomycin (GibcoBRL, France), 2.5 $\mu\text{g}/\text{mL}$ amphotericin B (GibcoBRL, France), and 20 mM HEPES (Sigma, France).

4.3.4. Effect of **2f-tartaric** on metabolic activity and viability of endothelial cells

As previously described [52], HUVEC were plated at 20,000 cells/cm² in 24 well plates in complete medium. After 24 h, the medium was changed and cells were cultured with **2f-tartaric** (0–100 μM) in RPMI 1640 medium supplemented with 2% heat inactivated fetal calf serum (SVF) during 24 h.

Metabolic activity (MTT assay): cells were incubated with 0.4 mg/mL of 3-[4,5-dimethylthiazol-2-yl]-2,5-diphenyl tetrazolium bromide (MTT) (Sigma, France) at 37 °C during 3 h. Formazan crystals were dissolved by dimethylsulfoxide (Fisher Scientific, France) and absorbance was measured at 570/630 nm (EL800 Universal microplate reader, Bio-Tek instrument, USA). Results are presented as percent of variation with values obtained for control

medium without **2f-tartaric** as reference (Means \pm SD, $n = 3$ in triplicate).

Viability (Hoechst assay): cells were lysed by freezing at -80°C . Cell lysates were incubated with $2\ \mu\text{g}$ of Hoechst 33258 (Sigma, France) during 1 h under agitation and the fluorescence intensity was measured ($\lambda_{\text{excitation}}$: 360 nm/ $\lambda_{\text{emission}}$: 460 nm, Berthold Twinkle LB970 system). Results are presented as percent of variation with values obtained for control medium without **2f-tartaric** as reference (Means \pm SD, $n = 3$ in triplicate).

Effect of DMSO on the viability of endothelial cells was evaluated after dilution in RPMI 1640 medium supplemented with 2% SVF.

4.3.5. Endothelial cell tube formation

As previously described [52], HUVEC were plated (90,000 cells/ cm^2) onto 24-well plate pre-coated with Matrigel[®] (BD Biosciences, France). After 1 h, media were removed and replaced by **2f-tartaric** (0–3 μM) in RPMI 1640 medium supplemented with 2% heat inactivated fetal calf serum and 50 ng VEGF during 24 h before HUVEC being fixed with 4% paraformaldehyde (Sigma, France). Photomicrographs (Nikon AZ100, Digital Sight DS-Q11Mc camera, Nikon, France) were taken after phalloidin-sulforhodamine staining (Fluoroprobes[®], Interchim, France). Area fraction of endothelial cells was calculated with NIS Element Software (Nikon, France) and represented as the area fraction of cells in relation to whole field. It was expressed as a percentage of variation with values obtained for control medium without VEGF and without **2f-tartaric** as reference (negative control) (Means \pm SEM, $n = 5$). For comparison purpose, Sunitinib (LC Laboratories, USA) was used as reference drug using the same protocol.

Funding sources

This study was supported by grants from the French 'Ligue Nationale contre le Cancer' and the 'Region Lorraine', a PhD grant to E.P. from the French 'Ministère de l'Enseignement Supérieur et de la Recherche' and from Italian Ministry of University and Research (MIUR Grant 2008F8T894_002 and 2008ZTN724_003, PRIN Grant 20105YY2HL). One of us (F.B.) acknowledge SapienzaUniversità di Roma (grant "Progetti per Avvio alla Ricerca" prot. C26N12JZCT).

Acknowledgments

The authors thank the staff of obstetric department of Nancy maternity hospital and pregnant women for providing umbilical cords.

Appendix A. Supplementary material

Supplementary data related to this article can be found at <http://dx.doi.org/10.1016/j.ejmech.2013.03.022>.

References

- [1] D. Ribatti, A. Vacca, B. Nico, L. Roncali, F. Dammacco, Postnatal vasculogenesis, *Mech. Dev.* 100 (2001) 157–163.
- [2] W. Risau, Mechanisms of angiogenesis, *Nature* 386 (1997) 671–674.
- [3] D.A. Walsh, L. Haywood, Angiogenesis: a therapeutic target in arthritis, *Curr. Opin. Invest. Drugs* 2 (2001) 1054–1063.
- [4] G.A. Fava, Affective disorders and endocrine disease. New insights from psychosomatic studies, *Psychosomatics* 35 (1994) 341–353.
- [5] L.P. Aiello, R.L. Avery, P.G. Arrigg, B.A. Keyt, H.D. Jampel, S.T. Shah, L.R. Pasquale, H. Thieme, M.A. Iwamoto, J.E. Park, et al., Vascular endothelial growth factor in ocular fluid of patients with diabetic retinopathy and other retinal disorders, *N. Engl. J. Med.* 331 (1994) 1480–1487.
- [6] M. Detmar, The role of VEGF and thrombospondins in skin angiogenesis, *J. Dermatol. Sci.* 24 (Suppl. 1) (2000) S78–S84.
- [7] J. Folkman, Anti-angiogenesis: new concept for therapy of solid tumors, *Ann. Surg.* 175 (1972) 409–416.
- [8] L.A. Liotta, P.S. Steeg, W.G. Stetler-Stevenson, Cancer metastasis and angiogenesis: an imbalance of positive and negative regulation, *Cell* 64 (1991) 327–336.
- [9] N. Ferrara, VEGF and the quest for tumour angiogenesis factors, *Nat. Rev. Cancer* 2 (2002) 795–803.
- [10] N. Ferrara, R.S. Kerbel, Angiogenesis as a therapeutic target, *Nature* 438 (2005) 967–974.
- [11] R.S. Kerbel, Tumor angiogenesis, *N. Engl. J. Med.* 358 (2008) 2039–2049.
- [12] N. Ferrara, H.P. Gerber, J. LeCouter, The biology of VEGF and its receptors, *Nat. Med.* 9 (2003) 669–676.
- [13] N. Almog, L. Ma, R. Raychowdhury, C. Schwager, R. Erber, S. Short, L. Hlatky, P. Vajkoczy, P.E. Huber, J. Folkman, A. Abdollahi, Transcriptional switch of dormant tumors to fast-growing angiogenic phenotype, *Cancer Res.* 69 (2009) 836–844.
- [14] M.A. Gimbrone Jr., S.B. Leapman, R.S. Cotran, J. Folkman, Tumor dormancy in vivo by prevention of neovascularization, *J. Exp. Med.* 136 (1972) 261–276.
- [15] S. Baka, A.R. Clamp, G.C. Jayson, A review of the latest clinical compounds to inhibit VEGF in pathological angiogenesis, *Expert Opin. Ther. Targets* 10 (2006) 867–876.
- [16] B.M. Klebl, K. Muller, Second-generation kinase inhibitors, *Expert Opin. Ther. Targets* 9 (2005) 975–993.
- [17] L. Sepp-Lorenzino, K.A. Thomas, Antiangiogenic agents targeting vascular endothelial growth factor and its receptors in clinical development, *Expert Opin. Invest. Drugs* 11 (2002) 1447–1465.
- [18] C.T. Supuran, A. Scozzafava, Protein tyrosine kinase inhibitors as anticancer agents, *Expert Opin. Ther. Patents* 14 (2004) 35–53.
- [19] P. Carmeliet, L. Moons, A. Luttun, V. Vincenzi, V. Compernelle, M. De Mol, Y. Wu, F. Bon, L. Devy, H. Beck, D. Scholz, T. Acker, T. DiPalma, M. Dewerchin, A. Noel, I. Stalmans, A. Barra, S. Blacher, T. Vandendriessche, A. Ponten, U. Eriksson, K.H. Plate, J.M. Foidart, W. Schaper, D.S. Charnock-Jones, D.J. Hicklin, J.M. Herbert, D. Collen, M.G. Persico, Synergism between vascular endothelial growth factor and placental growth factor contributes to angiogenesis and plasma extravasation in pathological conditions, *Nat. Med.* 7 (2001) 575–583.
- [20] N. Ferrara, K.J. Hillan, H.P. Gerber, W. Novotny, Discovery and development of bevacizumab, an anti-VEGF antibody for treating cancer, *Nat. Rev. Drug Discov.* 3 (2004) 391–400.
- [21] S.M. Wilhelm, C. Carter, L.Y. Tang, D. Wilkie, A. McNabola, H. Rong, C. Chen, X.M. Zhang, P. Vincent, M. McHugh, Y.C. Cao, J. Shujath, S. Gawlak, D. Eveleigh, B. Rowley, L. Liu, L. Adnane, M. Lynch, D. Auclair, I. Taylor, R. Gedrich, A. Voznesensky, B. Riedl, L.E. Post, G. Bollag, P.A. Trail, BAY 43-9006 exhibits broad spectrum oral antitumor activity and targets the RAF/MEK/ERK pathway and receptor tyrosine kinases involved in tumor progression and angiogenesis, *Cancer Res.* 64 (2004) 7099–7109.
- [22] R.J. Motzer, M.D. Michaelson, B.G. Redman, G.R. Hudes, G. Wilding, R.A. Figlin, M.S. Ginsberg, S.T. Kim, C.M. Baum, S.E. DePrimo, J.Z. Li, C.L. Bello, C.P. Thuermer, D.J. George, B.I. Rini, Activity of SU11248, a multitargeted inhibitor of vascular endothelial growth factor receptor and platelet-derived growth factor receptor, in patients with metastatic renal cell carcinoma, *J. Clin. Oncol.* 24 (2006) 16–24.
- [23] S. Faivre, C. Delbaldo, K. Vera, C. Robert, S. Lozahic, N. Lassau, C. Bello, S. Deprimo, N. Brega, G. Massimini, J.P. Armand, P. Scigalla, E. Raymond, Safety, pharmacokinetic, and antitumor activity of SU11248, a novel oral multitarget tyrosine kinase inhibitor, in patients with cancer, *J. Clin. Oncol.* 24 (2006) 25–35.
- [24] D. Strumberg, H. Richly, R.A. Hilger, N. Schleucher, S. Korfee, M. Tewes, M. Faghghi, E. Brendel, D. Voliotis, C.G. Haase, B. Schwartz, A. Awada, R. Voigtman, M.E. Scheulen, S. Seiber, Phase I clinical and pharmacokinetic study of the Novel Raf kinase and vascular endothelial growth factor receptor inhibitor BAY 43-9006 in patients with advanced refractory solid tumors, *J. Clin. Oncol.* 23 (2005) 965–972.
- [25] R. Rahman, S. Smith, C. Rahman, R. Grundy, Antiangiogenic therapy and mechanisms of tumor resistance in malignant glioma, *J. Oncol.* 2010 (2010) 251231.
- [26] J. Robert, L'angiogenèse, Application Médicale du GENE Collection, John Libbey Eurotext, 2009.
- [27] A. Garofalo, L. Goossens, P. Six, A. Lemoine, S. Ravez, A. Farce, P. Depreux, Impact of aryloxy-linked quinazolines: a novel series of selective VEGFR-2 receptor tyrosine kinase inhibitors, *Bioorg. Med. Chem. Lett.* 21 (2011) 2106–2112.
- [28] E. Hu, A. Tasker, R.D. White, R.K. Kunz, J. Human, N. Chen, R. Buerli, R. Hungate, P. Novak, A. Itano, X.X. Zhang, V. Yu, Y. Nguyen, Y. Tudor, M. Plant, S. Flynn, Y. Xu, K.L. Meagher, D.A. Whittington, G.Y. Ng, Discovery of aryl amino-quinazoline pyridones as potent selective, and orally efficacious inhibitors of receptor tyrosine kinase c-Kit, *J. Med. Chem.* 51 (2008) 3065–3068.
- [29] D.S. La, J. Belzile, J.V. Bready, A. Coxon, T. DeMelfi, N. Doerr, J. Estrada, J.C. Flynn, S.R. Flynn, R.F. Graceffa, S.P. Harriman, J.F. Larrow, A.M. Long, M.W. Martin, M.J. Morrison, V.F. Patel, P.M. Roveto, L. Wang, M.M. Weiss, D.A. Whittington, Y. Teffera, Z. Zhao, A.J. Polverino, J.C. Harmange, Novel 2,3-dihydro-1,4-benzoxazines as potent and orally bioavailable inhibitors of tumor-driven angiogenesis, *J. Med. Chem.* 51 (2008) 1695–1705.
- [30] Y. Miyazaki, S. Matsunaga, J. Tang, Y. Maeda, M. Nakano, R.J. Philippe, M. Shibahara, W. Liu, H. Sato, L. Wang, R.T. Nolte, Novel 4-amino-furo[2,3-d]

- pyrimidines as Tie-2 and VEGFR2 dual inhibitors, *Bioorg. Med. Chem. Lett.* 15 (2005) 2203–2207.
- [31] B.L. Hodous, S.D. Geuns-Meyer, P.E. Hughes, B.K. Albrecht, S. Bellon, J. Bready, S. Caenepeel, V.J. Cee, S.C. Chaffee, A. Coxon, M. Emery, J. Fretland, P. Gallant, Y. Gu, D. Hoffman, R.E. Johnson, R. Kendall, J.L. Kim, A.M. Long, M. Morrison, P.R. Olivieri, V.F. Patel, A. Polverino, P. Rose, P. Tempest, L. Wang, D.A. Whittington, H. Zhao, Evolution of a highly selective and potent 2-(pyridin-2-yl)-1,3,5-triazine Tie-2 kinase inhibitor, *J. Med. Chem.* 50 (2007) 611–626.
- [32] P.A. Harris, A. Boloor, M. Cheung, R. Kumar, R.M. Crosby, R.G. Davis-Ward, A.H. Epperly, K.W. Hinkle, R.N. Hunter 3rd, J.H. Johnson, V.B. Knick, C.P. Laudeman, D.K. Luttrell, R.A. Mook, R.T. Nolte, S.K. Rudolph, J.R. Szweczyk, A.T. Truesdale, J.M. Veal, L. Wang, J.A. Stafford, Discovery of 5-[[4-[(2,3-dimethyl-2H-indazol-6-yl)methylamino]-2-pyrimidinyl]amino]-2-methylbenzenesulfonamide (Pazopanib), a novel and potent vascular endothelial growth factor receptor inhibitor, *J. Med. Chem.* 51 (2008) 4632–4640.
- [33] R. Ragno, VEGFR-2 inhibitors. Ligand-Based, structure-based and 3-D QSAR studies as tools to design new small molecules, in: XXIII Congresso Nazionale della Società Chimica Italiana, Sorrento, Italy, 2009.
- [34] S. Hesse, E. Perspicace, G. Kirsch, Microwave-assisted synthesis of 2-aminothiophene-3-carboxylic acid derivatives, 3H-thieno[2,3-d]pyrimidin-4-one and 4-chlorothiopheno[2,3-d]pyrimidine, *Tetrahedron Lett.* 48 (2007) 5261–5264.
- [35] E. Perspicace, S. Hesse, G. Kirsch, M. Yemloul, C. Lecomte, Unexpected C–O bond formation in Suzuki coupling of 4-chlorothiopheno[2,3-d]pyrimidines, *J. Heterocycl. Chem.* 46 (2009) 459–464.
- [36] D. Thomae, E. Perspicace, S. Hesse, G. Kirsch, P. Seck, Synthesis of substituted [1,3]thiazolo[4,5-b]pyridines and [1,3]thiazolo[4,5-d][1,2,3]triazines, *Tetrahedron* 64 (2008) 9309–9314.
- [37] E. Perspicace, D. Thomae, G. Hamm, S. Hesse, G. Kirsch, P. Seck, Synthesis of substituted selenolo[3,2-d][1,2,3]triazines and [1,3]selenazolo[4,5-d][1,2,3]triazines, *Synthesis* (2009) 3472–3476.
- [38] M.D. Shults, B. Imperiali, Versatile fluorescence probes of protein kinase activity, *J. Am. Chem. Soc.* 125 (2003) 14248–14249.
- [39] E. Migianu, G. Kirsch, Synthesis of new thieno[b]azepinediones from α -methylene ketones, *Synthesis* (2002) 1096–1100.
- [40] H. Hartmann, J. Liebscher, A simple method for the synthesis of 5-aryl-3-amino-2-alkoxycarbonylthiophenes, *Synthesis-stuttgart* (1984) 275–276.
- [41] S. Kim, K.Y. Yi, Synthetic applications of di-2-pyridyl thionocarbonate as a dehydration, a dehydrosulfurization, and a thiocarbonyl transfer reagent, *Bull. Korean Chem. Soc.* 8 (1987) 466–470.
- [42] M.I. Crespo, L. Pages, A. Vega, V. Segarra, M. Lopez, T. Domenech, M. Miralpeix, J. Beleta, H. Ryder, J.M. Palacios, Design, synthesis, and biological activities of new thieno 3,2-d pyrimidines as selective type 4 phosphodiesterase inhibitors, *J. Med. Chem.* 41 (1998) 4021–4035.
- [43] O. Ottoni, R. Cruz, R. Alves, Efficient and simple methods for the introduction of the sulfonyl, acyl and alkyl protecting groups on the nitrogen of indole and its derivatives, *Tetrahedron* 54 (1998) 13915–13928.
- [44] V.O. Illi, Phase transfer-catalyzed N-sulfonation of indole, *Synthesis* (1979) 136.
- [45] G.M. Morris, R. Huey, A.J. Olson, Using AutoDock for Ligand–receptor Docking, *Curr Protoc Bioinformatics* (2008) Chapter 8, Unit 8 14.
- [46] I. Musmuca, A. Caroli, A. Mai, N. Kaushik-Basu, P. Arora, R. Ragno, Combining 3-D quantitative structure-activity relationship with ligand based and structure based alignment procedures for in silico screening of new hepatitis C virus NS5B polymerase inhibitors, *J. Chem. Inf. Model.* 50 (2010) 662–676.
- [47] F. Ballante, R. Ragno, 3-D QSAutogrid/R: an alternative procedure to build 3-D QSAR models. methodologies and applications, *J. Chem. Inf. Model.* 52 (2012) 1674–1685.
- [48] Z. Yang, K. Lasker, D. Schneidman-Duhovny, B. Webb, C.C. Huang, E.F. Pettersen, T.D. Goddard, E.C. Meng, A. Sali, T.E. Ferrin, UCSF Chimera, MODELLER, and IMP: an integrated modeling system, *J. Struct. Biol.* 179 (2011) 269–278.
- [49] R.D.C. Team, The R Foundation for statistical computing, (2002).
- [50] A.C. Wallace, R.A. Laskowski, J.M. Thornton, LIGPLOT: a program to generate schematic diagrams of protein–ligand interactions, *Protein Eng.* 8 (1995) 127–134.
- [51] E.A. Jaffe, R.L. Nachman, C.G. Becker, C.R. Minick, Culture of human endothelial cells derived from umbilical veins. Identification by morphologic and immunologic criteria, *J. Clin. Invest.* 52 (1973) 2745–2756.
- [52] V. Jouan-Hureau, C. Boura, J.-L. Merlin, B. Faivre, Modulation of endothelial cell network formation *in vitro* by molecular signaling of head and neck squamous cell carcinoma (HNSCC) exposed to cetuximab, *Microvasc. Res.* 83 (2012) 131–137.